University of Nevada, Reno

DESIGN AND FABRICATION OF A UNIVERSAL SOFT GRIPPER

A Thesis Submitted in Partial Fulfillment

of the Requirements for the Degree of Master of Science in

Mechanical Engineering

by

Amin Sabzehzar

Dr. Wanliang Shan / Thesis Advisor

August 2017

THE GRADUATE SCHOOL

We recommend that the thesis
prepared under our supervision by

AMIN SABZEHZAR

Entitled

Design and Fabrication of a Universal Soft Gripper

be accepted in partial fulfillment of the
requirements for the degree of

MASTER OF SCIENCE

Dr. Wanliang Shan , Advisor

Dr. Matteo Aureli , Committee Member

Dr. Mark Pingle , Graduate School Representative

David W. Zeh, Ph.D., Dean, Graduate School

August, 2017

ABSTRACT

Inspired from nature, soft robots capable of actively tuning their mechanical rigidity can rapidly transition between a broad range of motor tasks, from lifting heavy loads to dexterous manipulation of delicate objects. Reversible rigidity tuning also enables soft robotic actuators to reroute their internal loading and alter their mode of deformation in response to intrinsic activation. In this study, we demonstrate this principle with a three-fingered pneumatic gripper that contains programmable ligaments that change stiffness when activated with electrical current. The ligaments are composed of a conductive thermoplastic elastomer composite that reversibly softens under resistive heating. Depending on which ligaments are activated, the gripper will bend inward to pick up an object, bend laterally to twist it, or bend outward to release it.

Each finger consists of three PDMS phalanges that are attached with two Ecoflex joints. Three ligaments (strips of a cPBE-PDMS composite layer) are attached along the finger and are stimulated with electricity individually. When the high pressure air is injected in the hollow middle part of the finger, the finger will be bent in the opposite direction of the stimulated cPBE-PDMS element (softer wall). This enables the gripper's fingers to grab and twist objects with different sizes and shapes.

All of the gripper motions are generated with a single pneumatic source of pressure and are controlled with an electrical board. The ability to incorporate electrically programmable ligaments in pneumatic or hydraulic actuators has the potential to enhance versatility and reduce dependency on tubing and valves. In this study, an activation/deactivation cycle can be completed within 15 s.

ACKNOWLEDGEMENTS

First all of all, I would like to express the deepest gratitude to my advisor and mentor, Dr. Wanliang Shan, for providing me the opportunity to work on the various projects and for the encouragement and guidance through the course of my two-year graduate study at University of Nevada, Reno. I deeply appreciate his efforts of helping me develop my skills as an independent scientist. All of these will surely benefit me throughout my future career and life.

I would especially like to thank my thesis committee members, Dr. Matteo Aureli and Dr. Mark Pingle, for serving as the committee members and providing me with intellectual comments and suggestions. I am indebted to a host of other people, in particular, Dr. Henry Fu and Dr. Faramarz Gordaninejad for their help and being the Assistant of Instruction for the courses they taught at University of Nevada, Reno. I would like to thank Mechanical Engineering Department of University of Nevada, Reno for the support in every step throughout the Master's program and for making it enjoyable.

I would also like to thank my peers at Shan Research Group at University of Nevada, Reno, Mr. Amir Mohammadi Nasab, Mr. Milad Tatari, and Mr. Patrick Stampfli for their suggestions and discussion on my research work. I am grateful to my peers at teacher assistants' office, Dr. Justin Ferranto and Mr. Syed N. Ahsan for their support and help during my research.

Finally, I owe my sincere appreciation to my family, Mr. Abbas Sabzehzar, Mrs. Zohreh Sahraei, Mrs, Samira Sabzehzar, and specially my brother, Dr. Saman Sabzehzar, for the encouragement and support they provided along the course. They were there together with me to persevere the adversities and to enjoy the happiness of every bit of progress and suc-

cess. Without their care and support, arriving at the finish line of the long journey of M.Sc. study would be unimaginable.

Table of Contents

List of Figures

Chapter 1

Introduction

1.1 Background

Soft robotics was born from the thought of bio-inspired design, which is about learning the concepts of natural organisms and utilizing these concepts in design and fabrication of high performance materials and structures. Although conventional robotics is precise, powerful, and highly specialized, they have limited working space and unsafe interaction with humans. Unlike conventional robots that are made of rigid materials, soft robots are made of deformable matters such as fluids, gels, and elastomers that can match with the elastic properties of natural tissues [19]. In different applications, it is shown that conventional robots equipped with soft bodies are more robust, adaptable, and safer comparing to completely rigid ones [20].

Design and application of soft robotic is closely associated with the improvement of soft materials. Soft matter engineering is a new field of science to study the behavior of

materials capable of large deformation. Stiffness in soft materials can be controlled in different ways including the use of external air pressure, electricity, or vacuum machines. In some other applications, deformable behavior of soft materials enables the fabrication of soft devices like wearable gloves, artificial muscles, and medical robotics [10] [11].

1.1.1 Soft Wearable Devices and Tissues

Iskin is a soft device that is worn on human body, like gloves or watches, and acts as an input interface for human-computer interactions. A very thin, flexible, and stretchable Iskin sensor is capable of performing skin-like functions. These sensors can measure the magnitude of the pressure with two embedded electrodes that are overlaid and held apart in between of three elastomeric layers. Iskin sensors with different custom-shaped formations are worn on different parts of body as a touch input to control external devices [3].

Park et al. fabricated a hyper-elastic pressure sensor by embedding silicone rubber with microchannels of conductive liquid alloy, Eutectic Gallium Indium (EGaIn) [21]. Change in electrical resistance measures the magnitude of surface pressure. In another work, a capacitive microfluidic sensor was fabricated consisting of four flexible elastomer layers with two inner arrays of microfluidic channels filled with Galinstan [1]. This flexible microfluidic normal force sensor skin is calibrated to measure low frequency dynamic normal forces ranging from 0 to 2.5 N (Figure 1.1).

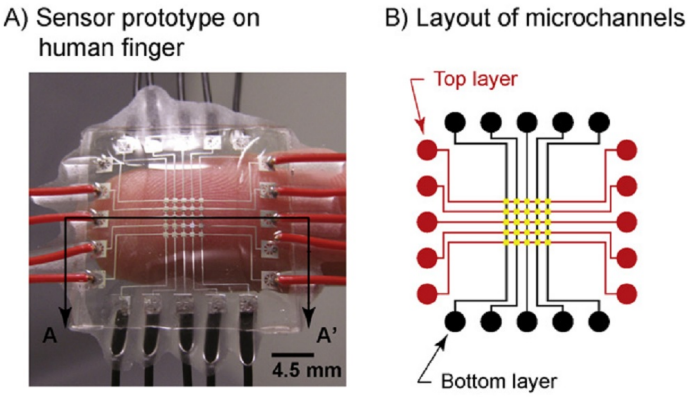

Figure 1.1: Normal force sensing skin. (a) Transparent polydimethylsiloxane (PDMS) embedded with Galinstan (b) Two wire paths overlapped, horizontally (red) on the top and vertically (black) at the bottom [1].

Like Iskin, Electronic skin (E-skin) is human-like skin capable of providing augmented performance both in superior spatial resolution and thermal sensitivity [22]. E-skin was first introduced by Lumelsky, in 2001, by designing a flexible array of sensors that can be used to cover the entire surface of a machine or even a part of a human body [23] [24]. Later, Roberts et al. introduced a soft-matter sensor that can measure the elastic normal and shear deformations. This potentially body-mounted sensor is a sheet of elastomer that is embedded with plate capacitors. The pressure or the shear stress changes the distance or overlaps between the capacitors. The measurement of the change is calibrated to calculate the normal force and shear deformations (Figures 1.2 and 1.3) [2].

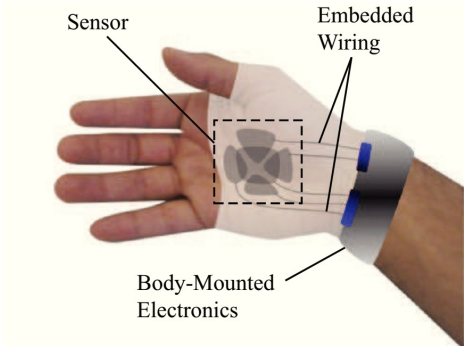

Figure 1.2: Glove with a soft-matter sensor to measure surface tractions on the palm [2].

Figure 1.2 proposes a sensor consisting of Ecoflex and EGaIn layers. It has the sensitivity of 500 μm and 5 kPa for the 2D shear and pressure deformations, respectively. Figure 1.3 illustrates the geometry and functioning of this sensor.

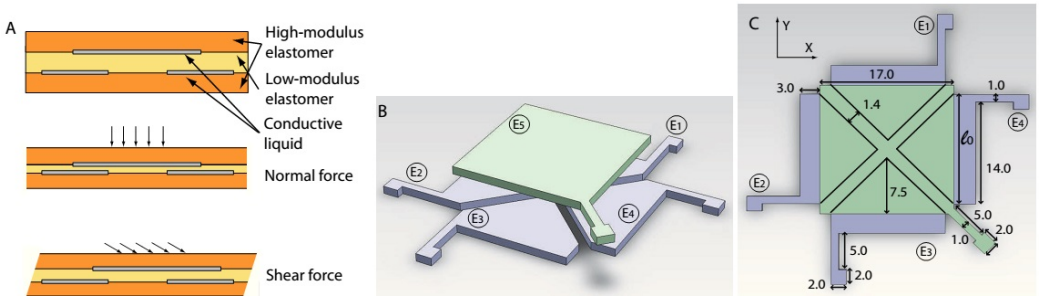

Figure 1.3: (A) Soft sensor layers and deformation under normal force and shear stress. (B) Alignment between the capacitors (C) Electrode dimensions (in mm) [2].

In 2015, Weigel et al. published their work on a novel class of skin-worn materials that are used as an interface on human skin, known as Visually Customizable On-Body Touch Sensors for Mobile Computing. These stretchable materials were produced in different shapes to be worn on human finger, ear, and wrist. As shown in Figure 1.4, these skin-worn materials were designed as a finger strap to manage incoming calls and extension for wearable devices. The fabrication consists of embedding three layers of PDMS with two layers

of carbon-filled PDMS (cPDMS) as transmitting and receiving electrodes in between. Two layers of cPDMS work as a capacitor that senses the external pressure and the three other layers of PDMS as stretchable seals (Figures 1.4 and 1.5) [3].

Figure 1.4: ISkin can be worn directly on the skin. Wigel et al. presented (from left to right) FingerStrap, one-handed control of telephone calls; extensions for wearable devices; SkinStickers, input surface for a music player attached; a click wheel on the back of the hand; and a headset control behind the ear [3].

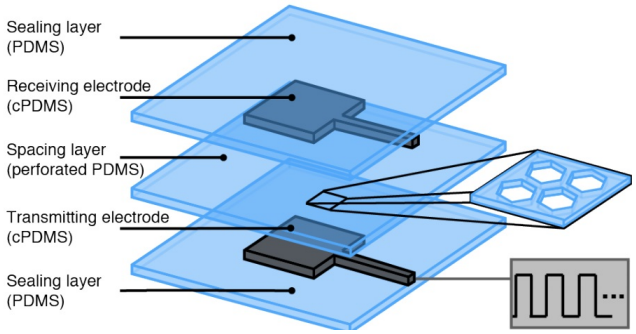

Figure 1.5: Schematic of Iskin touch layers [3].

Soft materials also have applications in the field of soft-matter electronics. This field of study focuses on the fabrication of a thin film of soft materials embedded with electrically conductive fluids, gels, and pastes. Lu et al. fabricated soft electronic devices composed of cPDMS and EGaIn embedded in a thin sheet of soft silicone elastomer. This is a series of rapid and inexpensive methods to produce soft sensors and circuits in minutes using a CO_2 laser. CO_2 laser is used to directly pattern the thin film of cPDMS and liquid-phase EGaIn alloy on the elastomer [4].

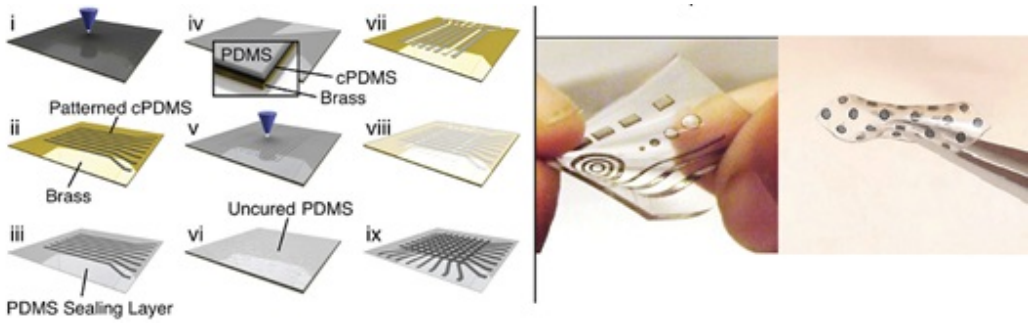

Figure 1.6: Steps to fabricate a resistive tactile sensor composed of multilayer cPDMS [4].

In other studies, soft sensors were fabricated to work in stretchable condition. Kim et al. fabricated an interconnected multiaxial stretchable structure using a microfluidic injection technique [25]. In this study, they used PDMS microchannels coated with a gold wetting layer with less than 0.02 Ω resistance variation for 180° bending. An electro-mechanical sensor was fabricated by Cheng et al. to remotely detect repeated high tensile dynamic strains over very large surfaces or movable parts [26]. This sensor consists of two layers of liquid metal alloy that are filled inside microfluidic channels in an elastomer matrix. Park et al. introduced an elastic conductive composite for fabricating stretchable electronic devices [5]. They classify the works in five steps of fabrication, as shown in Figure 1.7.

Another group of wearable soft devices were specially designed for high quality wireless communication. Jeong et al. described the microfluidic approach, based on the printed circuit board technology, to fabricate stretchable electronics to combine various sensors on human bodies and organs [6]. This method of manufacturing allows for large cross section conductors which can handle large stretching. They described their approaches in two categories of tape transfer printing and device fabrication, shown in Figure 1.8. This new approach enables manufacturers to mount radio frequency identification (RFID) tags on a

printed stretchable device.

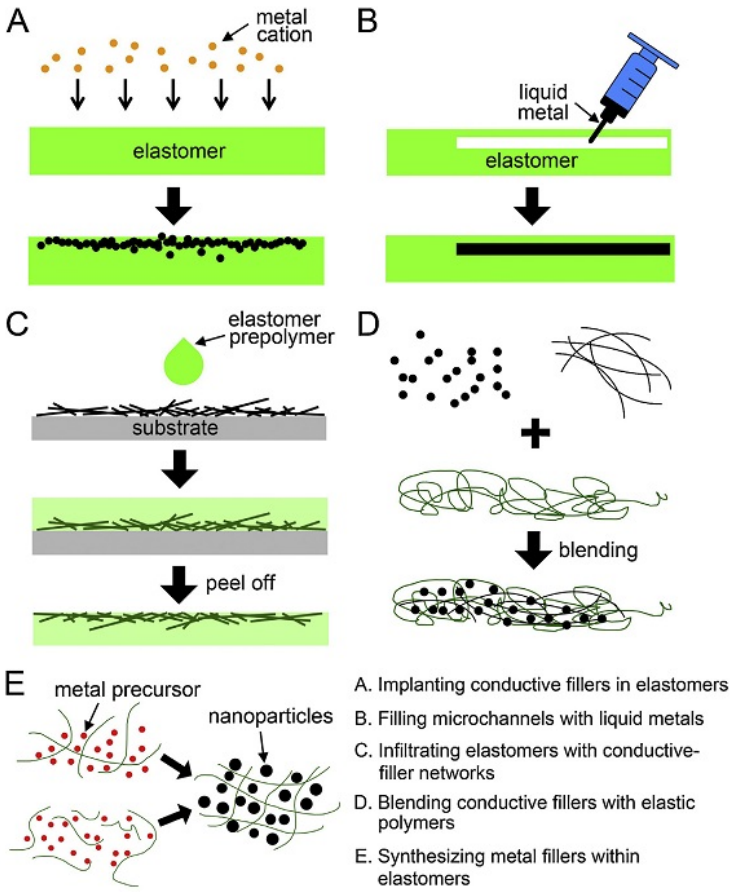

Figure 1.7: Schematic illustration of designing a conductive composite elastomer [5].

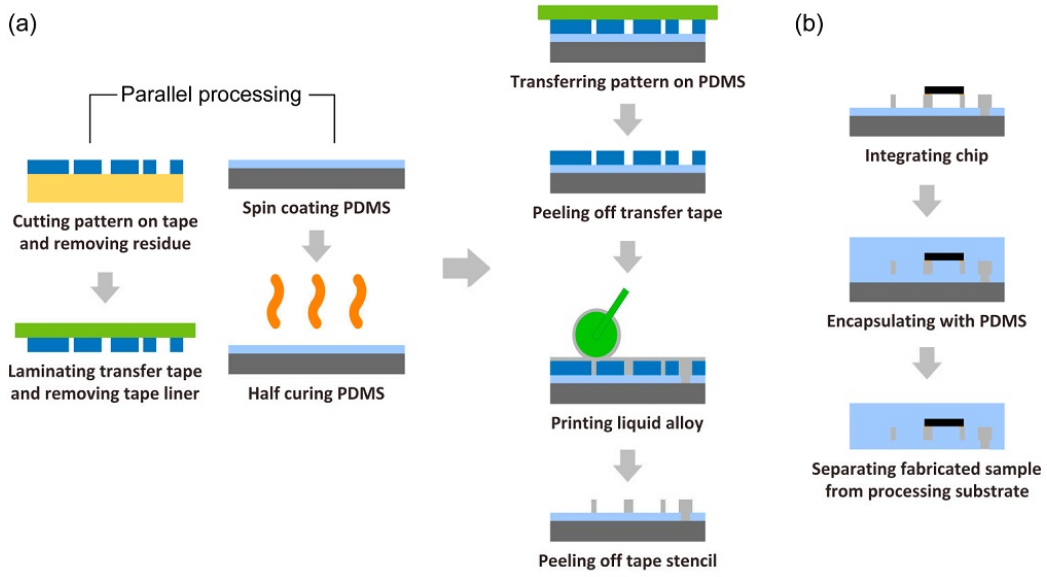

Figure 1.8: Processing steps for (a) tape transfer printing, and (b) device fabrication [6].

Beyond the application of soft materials to fabricate wearable devices and flexible electronics, these materials were used to fabricate tunable stiffness tissues and fully or partially soft bodies in robotics. Ou et al. introduced jamSheets, thin interface with tunable stiffness, to fabricate weaving structures, jamming shoes, stiffness changing displays, and deformable furniture, as shown in Figure 1.9 [7].

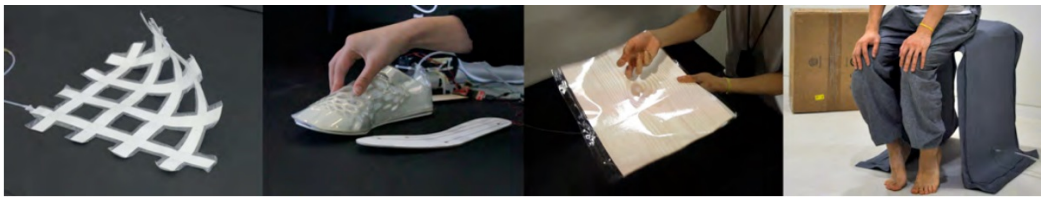

Figure 1.9: Weaving structure of materials with tunable stiffness [7].

1.1.2 Rigidity Tunable Materials

With the rapid growth of soft robotic applications, there are increasing demands for high performance soft components and structures that can be integrated with soft robotic systems. Among these, materials with tunable stiffness are highly desirable in particular. Many engineers and scientists have been working on variable stiffness materials to address potential needs and applications for automotive design [27], medicine [28], aeronautics [29], construction [30] and robotics [31].

Due to the considerable interest in the use of variable stiffness materials, many studies have been done on controllable stiffness beams with multi-layered structures. In 2007, a multi-layered composite was introduced consisting of a base beam, a soft cover layer, and a polymer layer in between [8]. The stiffness of the integral unit changes by coupling and decoupling of the cover layer from the base beam with an ultra-thin electric heating blanket. This blanket is embedded in the system to control the shear modulus of the polymer layer by changing the temperature.

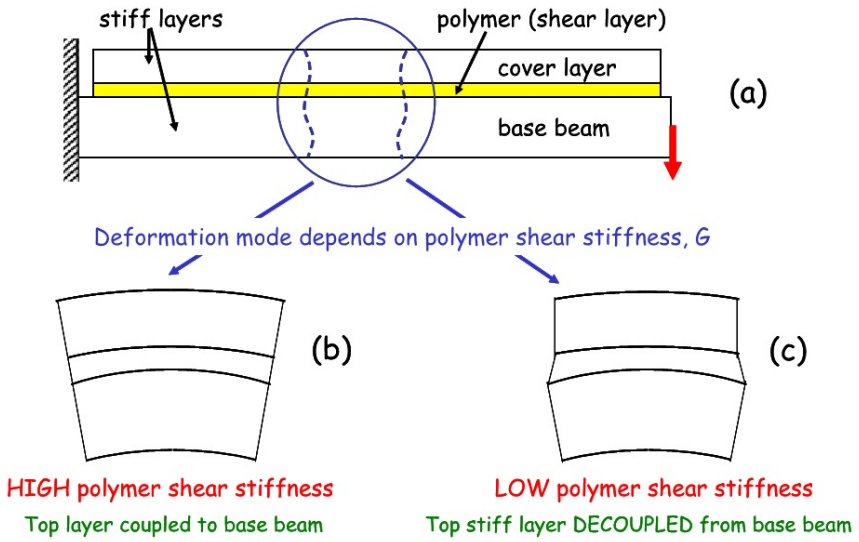

Figure 1.10: (a) Schematic representation of a multi-layered beam. (b and c) Deformation modes corresponding to high and low polymer shear moduli [8].

In another study, the stiffness of a beam was controlled by electric fields between the main element and stiffening elements [32]. Later in 2010, a controllable stiffness beam was realized by coupling and decoupling between polymer layers, affixed to the surface of a base beam [33]. When the polymer is heated, it undergoes glass transition and the effective shear modulus of the beam is decreased.

McEvoy and Correll proposed a composite structure with permanent geometry and tunable stiffness [9]. They fabricated a thermal based variable stiffness structure, in which a polycaprolactone rod is equipped with heating elements and thermistors. When the local region is heated up to a specific temperature, external moment deforms the whole structure to the desired shape. This composite is used to fabricate shape changing units such as multi-functional furniture or aerodynamic surfaces on boats, cars, and aircrafts.

Figure 1.11: Application of thermally shape changing materials [9].

In another study, a tunable stiffness device was controlled with external electricity. Wissman et al. proposed the Dielectric Elastomer Actuator (DEA) that is fabricated from EGaIn embedded between the layers of PDMS [34]. Saddle-like geometry is induced by applying voltage to the liquid metal electrodes. In other words, residual stresses in the dielectric and sealing layers of PDMS cause the DEA to deform into a saddle-like geometry. Experimental results verified the dependency of bending curvature on the applied voltage.

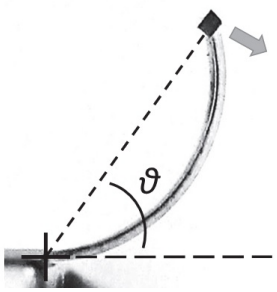

Figure 1.12: Soft-matter PDMS-GaIn DEA composite after bending.

Shan et al. embedded a thin sheet of phase-changing alloy, Field's metal, in an elas-

tomer to design a soft composite with tunable elastic rigidity. The Field's metal is rigid in room temperature and the composite remains rigid. Once Joule heating melts the Field's metal at a temperature higher than 62 °C, the elastomer stretches and bends freely under external moments. Joule heating decreases the elastic modulus of the composite by four orders of magnitude [10]. Figure 1.13 shows the working mechanism of this composite.

Shan et al. also generalized this multi-layered design of soft composites with tunable elastic rigidity and investigated their performances numerically. This class of elastomer based composites are embedded with Thermally-Responsive Materials (TRM). The TRM layer reversibly changes its rigidity by absorbing resistive heating through an embedded layer of liquid-phase Joule heater [35]. Figure 1.14 shows the dependency of activation time on input power for different combinations of rigidity tunable materials and elastomer matrix materials. Based on the figure, PDMS or other similar elastomers embedded with Field's metal are the best candidate for applications with allowance of slower activation time and high performance. Meanwhile, VHB is preferable for applications that need fast activation over drastic rigidity change. But this design overall lacks the ability to reduce the activation time to seconds.

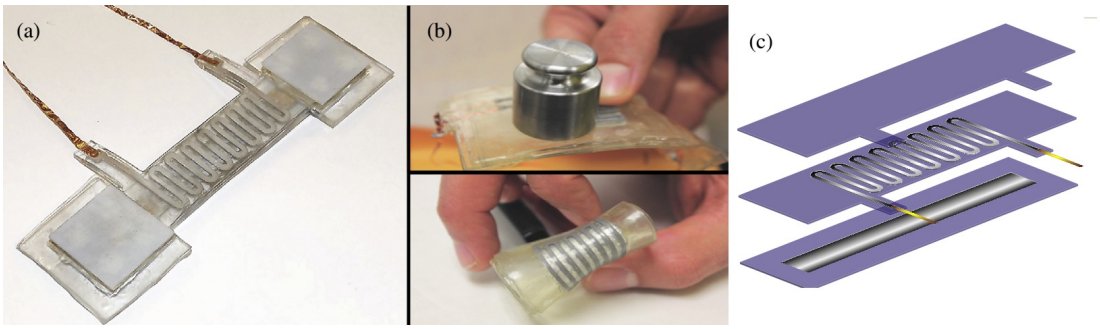

Figure 1.13: (a) Stiffness tunable composite of Field's metal strips embedded in elastomers. (b) The composite softens when electrically activated. (c) The composite composed of a (top) elastomer sealing layer, (middle) liquid-phase Joule heating element, and (bottom) thermally activated layer of Field's metal [10].

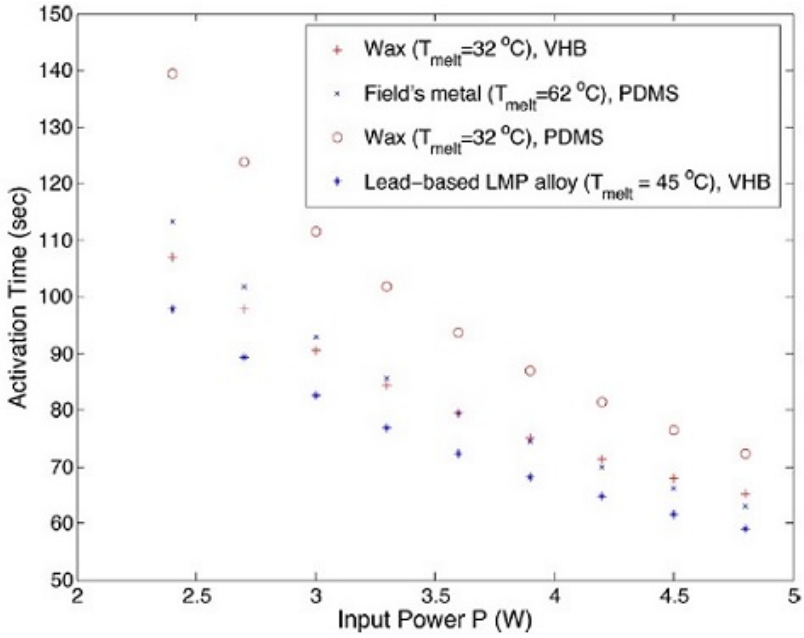

Figure 1.14: Predicted activation time of various thermally responsive materials and elastomers depending on power input [10].

In order to improve the response time of previous approaches, Shan et. al developed an electrically powered control mechanism [11]. In this study, Conductive Polypropylene Based Elastomer (cPBE), a propylene/ethylene copolymer with a network of structured carbon black, is rigid in its natural state and gets softer when electrically activated. This

composite simulates the natural skeletal muscle that requires rigidity tuning to accomplish its various functionalities. Figure 1.15 demonstrates the change in tunable stiffness of the composite before and after activation. Using this design, the activation time of the composite is down to a few seconds.

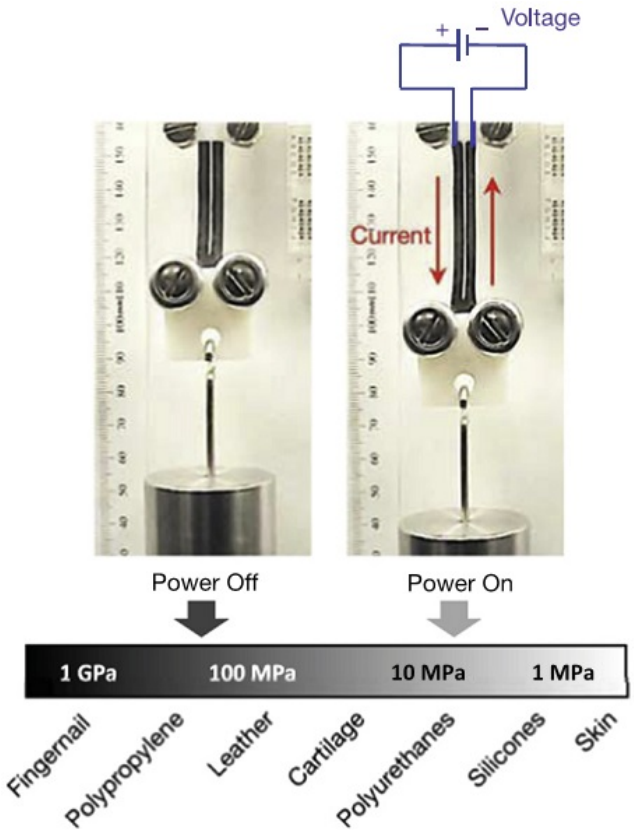

Figure 1.15: Rigidity tuning is accomplished with a cPBE-PDMS composite being stimulated electrically [11].

Schubert et al. improved previous works by developing variable stiffness composites with embedding rigid Low-Melting-Point-Alloy (LMPA) microstructure in PDMS [12]. Direct Joule-heating causes LMPA transition between rigid and soft states, which controls the variable stiffness of the composite by more than 25 times. They fabricated micro-scale channels and then needle-injected melted LMPA into it at elevated temperature. This com-

posite changes its stiffness very fast (in less than 1 sec) thanks to the small size of the channel.

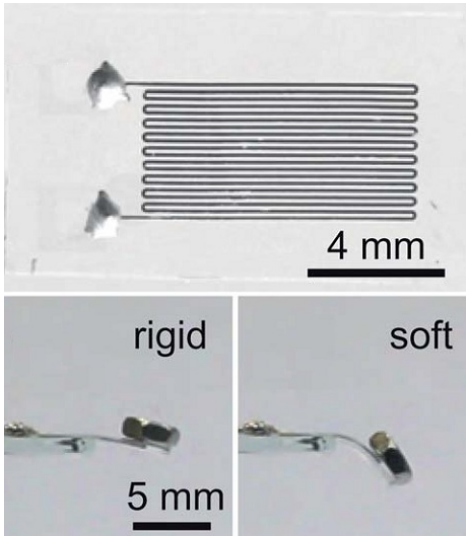

Figure 1.16: Variable stiffness composite beam of LMPA tracks embedded in PDMS [12].

Later in 2014, a wearable fabric with variable stiffness was fabricated from shape memory materials [13]. In this study, thin wires of shape memory alloy were coated with Shape Memory Polymer (SMP) via a quasi-continuous feed-through process. The stiffness is controlled thermally.

Figure 1.17: Wearable tunable stiffness fabric made from shape memory alloy [13].

1.1.3 Recent Development of Soft Robotic Grippers

Traditional grippers are mostly rigid structures with limited working space. These can be found in robotic manipulators that are used for assembly lines and machine tending. These manipulators are always fixed to ground and caged for the safety of human workers. By utilizing soft materials and fabrication of soft grippers, the Degrees Of Freedom (DOF) are increased and grippers are capable of doing delicate tasks in more complicated environment [36].

Robinson et al. and Simaan et al. presented a review of continuum and snake-like bending robots as an example of soft robotics [37] [38]. In 2009, a few studies were conducted in order to fabricate under-actuated mechanism in which the number of actuators were less than DOF [39].

Later, Yoshimi et al. presented a two-fingered soft robotic hand with a soft nail that can pick up a sheet of paper or a plastic card. They used the proposed approach to equip a home service robot. This robot consists of a hand, flexibe fingers and pressure sensors and is capable of picking up flat sheets of materials with different sizes [14].

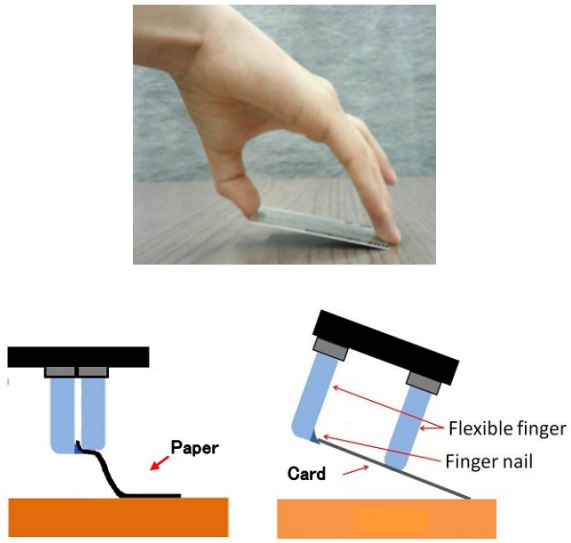

Figure 1.18: Comparing (up) human hand handling a card and (down) a two-finger parallel soft gripper handling a card [14].

Brown et al. presented a universal robotic gripper based on jamming of granular materials [15]. In their approach, the gripper is soft and deforms around the object when not actuated. By air evacuation, the object is locked and can be manipulated with the now-rigid gripper. Figure 1.19 D shows how this gripper works.

Ginnaccini et al. addressed the problem of a grasping device to accommodate handling objects with different shapes and sizes by presenting a low-cost elephant-trunk-shape soft gripper [16]. Their soft gripper consists of an empty shell with a silicone tube and cables

inside the shell. These cables bend the empty shell to grab objects with different sizes (Figure 1.20).

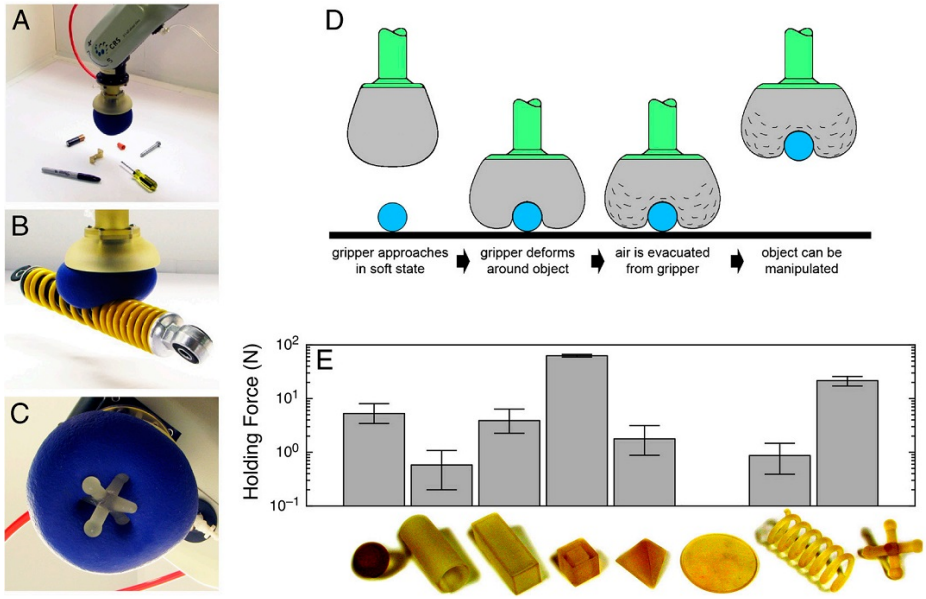

Figure 1.19: The efficiency of universal soft gripper to handle various objects with variable holding forces [15].

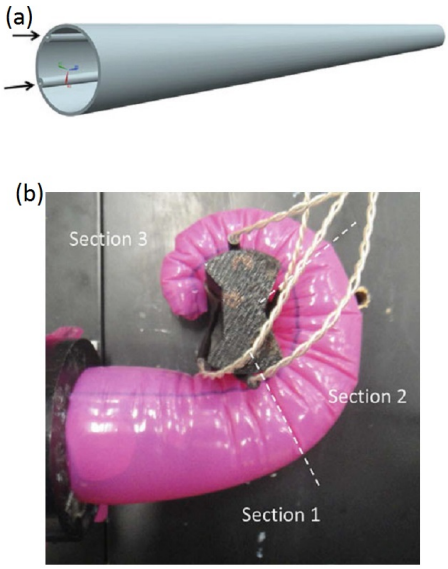

Figure 1.20: (a) Software model of an empty shell with silicone tubes. (b) The gripper has three working sections [16].

Figure 1.20 shows three different sections of the soft gripper including the base of the gripper, the middle part and the tip. Two twisted white wires are attached to the object in order to measure the applied force on the object surface. The internal side of the gripper has the concertina wall to bend and grab the object while the external side has no folds.

Araromi et al. presented a gripper made of rollable dielectric elastomer to remove active debris of the decommissioned nano-satellite [17]. The proposed soft gripper comes with mechanically resilient actuators and is capable of manipulating objects with different shapes and sizes. Figure 1.21 shows the schematic working scenario of a dielectric elastomer with Minimum Energy Structure (MES). The gripper is actuated by applying high voltage and deactivated by cutting the voltage off.

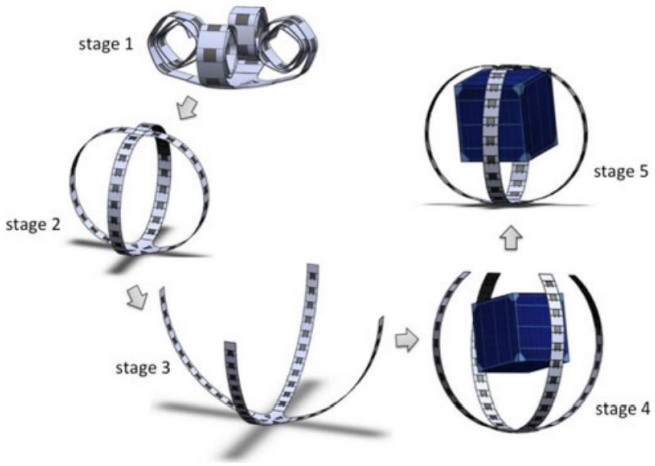

Figure 1.21: Working scenario of a dielectric elastomer minimum energy structure by applying high voltage electricity [17].

This dielectric gripper has four soft bonds of PDMS composite with a rigid plastic holder. Figure 1.22 shows the fabrication process of the MES; (a) On the left, a prestretched PDMS membrane was bonded to a rigid plastic holder with Kapton tape, on the right, an inextensible, but flexible, frame was printed with a hatched pattern on its surface; (b) Using a double-sided transparent tape, the flexible frame was bonded to the PDMS membrane surface. Then, the frame-membrane structure was released from the plastic holder; (c) First minimum energy equilibrium state of the MES; (d) Second equilibrium state of MES. The region shaded in green in the MES actuator is covered by a compliant electrode [17].

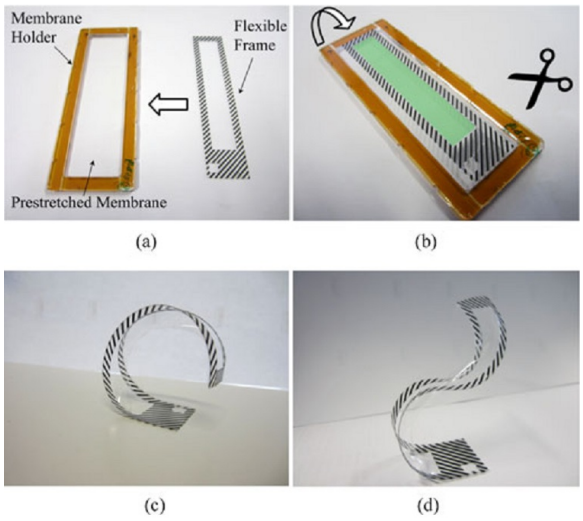

Figure 1.22: An example of MES [17].

Soft robotics is in a great demand for surgical tools applications and exploration robots. Firouzeh et al. presented an intuitive design to address the requirements for a locking mechanism with high DOF for manipulators with surgical purposes [18]. They used the probabilistic technique to determine the minimum number of active joints to achieve a desired posture. Their robot consists of two tendons controllable with two motors and SMP layers along the actuator. Shown in Figure 1.23, two stepper motors drive tendons in order to actuate each of the four folding joints.

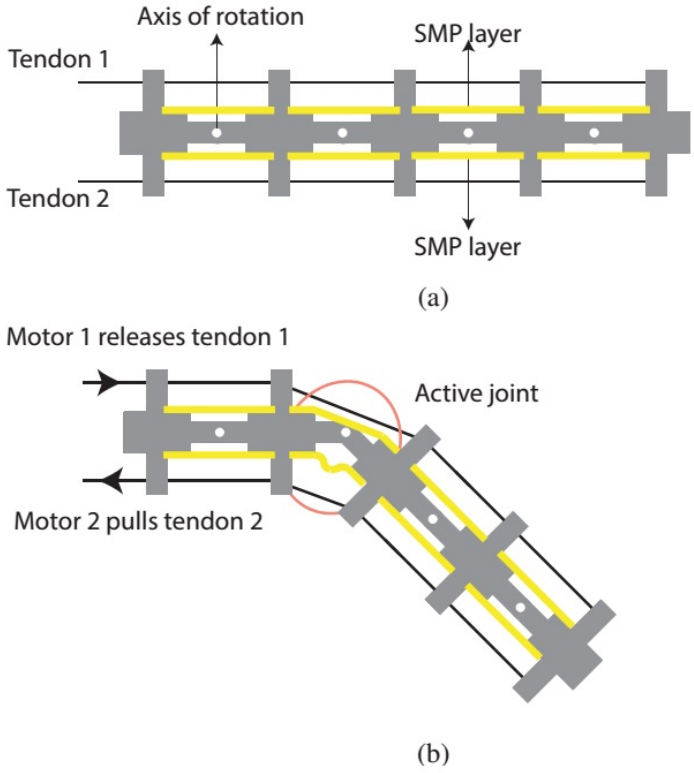

Figure 1.23: The working principle of an under-actuated robotic arm [18].

Each fold can be activated to bend the whole gripper in the desired direction. Figure 1.23 (b) depicts how the second joint can be bent in a desired direction by activating the second fold while keeping other folds stiff. Folds were fabricated from two composite layers of SMP with embedded heater in between (Figure 1.24).

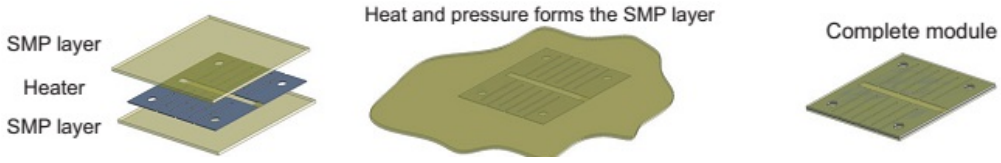

Figure 1.24: Fabrication method of a three-layer composite of SMP with an embedded heater [18].

1.2 Unresolved Issues and Scope of the Work

Inspired by nature, many soft grippers have been designed using pneumatic actuation mechanisms. In these soft grippers, mechanical asymmetry created by air pressure controls the bending motion of an individual finger, which is used collectively to generate the grasping motion of the gripper. For example, shown in Figure 1.25 (a), a pneumatic soft gripper consisting of variable number of fingers was attached to a single pneumatic channel. The sidewall of the pneumatic fingers was fabricated from two elastomeric halves with different rigidity [40]. Bending in finger was achieved when pressurized, due to the mechanical asymmetry of sidewall. Magnetic joints were used to assemble multiple modules of the soft robot.

In another study, a pneumatic universal robotic gripper was introduced based on jamming of granular materials, which is able to pick up objects with a wide range of sizes and shapes (Figure 1.25 b) [15]. Because they are soft, these group of pneumatically activated soft grippers can grasp a broad range of objects with a single motion. However, more sophisticated manipulation typically requires a dedicated pump or valve for each additional grasping mode or DOF.

In another group of studies, soft actuators were designed with electrically activated dielectric thin films embedded in elastomeric matrix. For example, Araromiet et al. introduced an electrically activated gripper based on prestretched dielectric elastomers [17]. The gripper consists of four fingers, which are prestretched dielectric elastomers bonded on a flexible frame (Figure 1.25 c). The bending angle can be tuned by high voltage input. In another study, a soft gripper was introduced, in which stiff fibers are embedded in a di-

electric elastomer film for wrapping motion generation (Figure 1.25 d) [41].

This group of soft grippers with prestretched elastomer membrane, patterned compliant electrodes, or two passive silicone layers, can pick up a wide range of objects including fragile and deformable ones. However, the high voltages required for these grippers (up to 10 kV) can sometimes pose safety issues and impose restrictions on the operating environment.

Other than pneumatically and electrically activated grippers described above, soft grippers based on the combination of two or more mechanisms have also been introduced. For example, to pick up objects with flat surfaces, Yoshimiet et al. designed a soft gripper consisting of two parallel soft fingers with a soft nail mounted on one of the fingers (Figure 1.25 e) [14]. Chenget et al. designed and fabricated an elephant trunk-shaped gripper that works with an evacuation pump and tension cables [42]. Giannacciniet et al. also introduced an elephant trunk-shaped gripper that picks up and holds roughly cylindrical objects (Figure 1.25 f and g) [16]. Although using the combination of mechanisms improved fabrication and functionality of soft grippers, the mentioned issues for pneumatically and electrically soft grippers still exist. More than that, none of the mentioned grippers are able to twist an object.

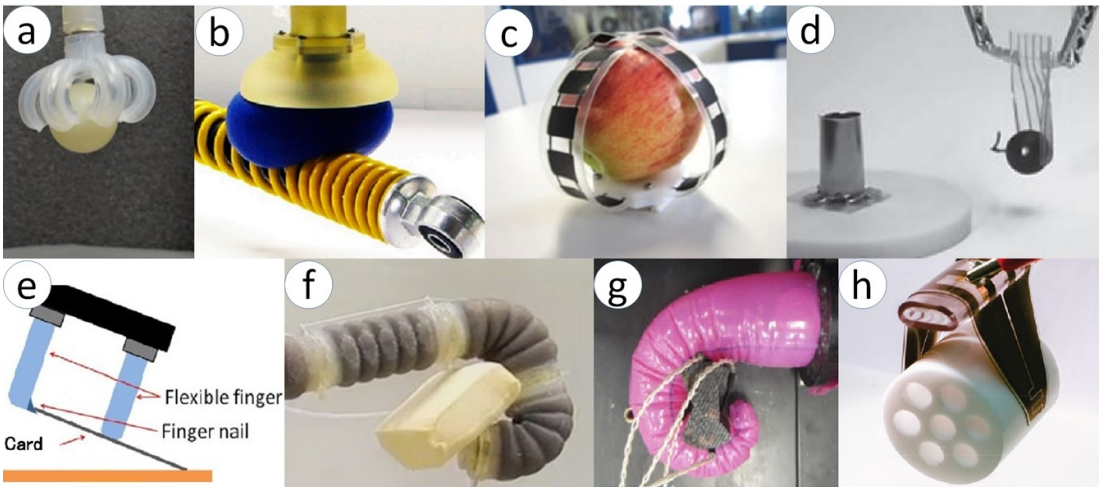

Figure 1.25: Different approaches to fabricate soft grippers.

To address aforementioned issues and enhance soft grippers efficiency, we have introduced a soft gripper that consists of three soft fingers attached to a rigid fixture. The proposed soft gripper, which works with single air pressure input and single electric supply, is capable of moving its fingers individually. This characteristic enables the gripper to pick objects with arbitrary shapes, and even more than that, to twist objects.

1.3 Organization of Thesis

In Chapter 1, the thorough overview of soft matter studies was presented with the focus on soft devices, novel soft engineering materials with tunable rigidity, and recent studies in the field of soft grippers. Then we stated how our gripper has improved the functionality of soft grippers and how it has addressed previous drawbacks.

In Chapter 2, a complete fabrication guide is presented step by step. The first step starts

with choosing the right materials and then design and fabrication of the finger's components. At the end, the assembly process and considerations are presented.

Later in Chapter 3, different test platforms are designed and implemented to test the mechanical functionality of the finger. These mechanical measurements are important to better understand the limitations of our gripper and to validate our theoretical results.

In Chapter 4, more in depth tests are done in order to: 1. challenge the soft gripper to pick up objects with different sizes and shapes in practice 2. evaluate the functionality of our gripper with FEA, and 3. measure the functionality of our gripper for twisting an object.

Finally in Chapter 5, we state the conclusions of this work, discuss the directions of future work, and provide perspectives on research in this general area of soft robotics.

Chapter 2

Design, Materials, and Fabrication

2.1 Overview

The soft fingers are made of silicone elastomers, Sylgard 184 PDMS and Ecoflex, as well as three cPBE-PDMS rigidity tunable multifunctional composites as ligaments. Each finger is composed of three phalanges made of PDMS and two joints made of Ecoflex similar to the human hand fingers. Both the phalanges and the joints are hollow such that each finger has a hollow chamber inside. There are three extensor ligaments made of cPBE-PDMS rigidity tunable elastomers positioned axisymmetrically around the finger sidewall; this feature provides the capability of bending in three as well as the reverse directions for the soft finger, enabling it to bend with even more flexibility than human fingers.

When its hollow chamber is inflated, the soft finger tends to expand in both the radial and the axial directions. Since the ligaments pose constrains for axial expansion of the finger, expansion mostly occurs in the radial direction. Furthermore, since the Ecoflex joints

are about 20 times softer than the PDMS phalanges, the expansion mostly occurs in the joints. Due to the symmetry in geometry and mechanical properties of the finger, the axial force will be equally balanced among the three ligaments. The radial forces applying on the inner surface of a symmetric chamber are in balance as well.

When one of the ligaments is activated, its rigidity decreases by about 35X. This disrupts the original symmetry in mechanical properties of the soft finger and causes the activated ligament to extend more than the nonactivated pair. Once the activated strip starts extending, the distal phalange will tilt toward the original axis of symmetry of the finger chamber, in the bending symmetry plane of the activated strip. The finger will continue to bend until it reaches a configuration where force balance in the bending symmetric plane of the activated ligament is reached again. Thus, by selectively activating different combinations of the ligaments, different manipulations such as grasping, releasing, and twisting can be achieved by the gripper.

To restore the finger to its original configuration before activation, the air pressure inside the hollow finger should be decreased to atmospheric pressure while the ligaments are still in activated state such that they can return to their original length due to the hyperelasticity of the PDMS component of the cPBE-PDMS composite.

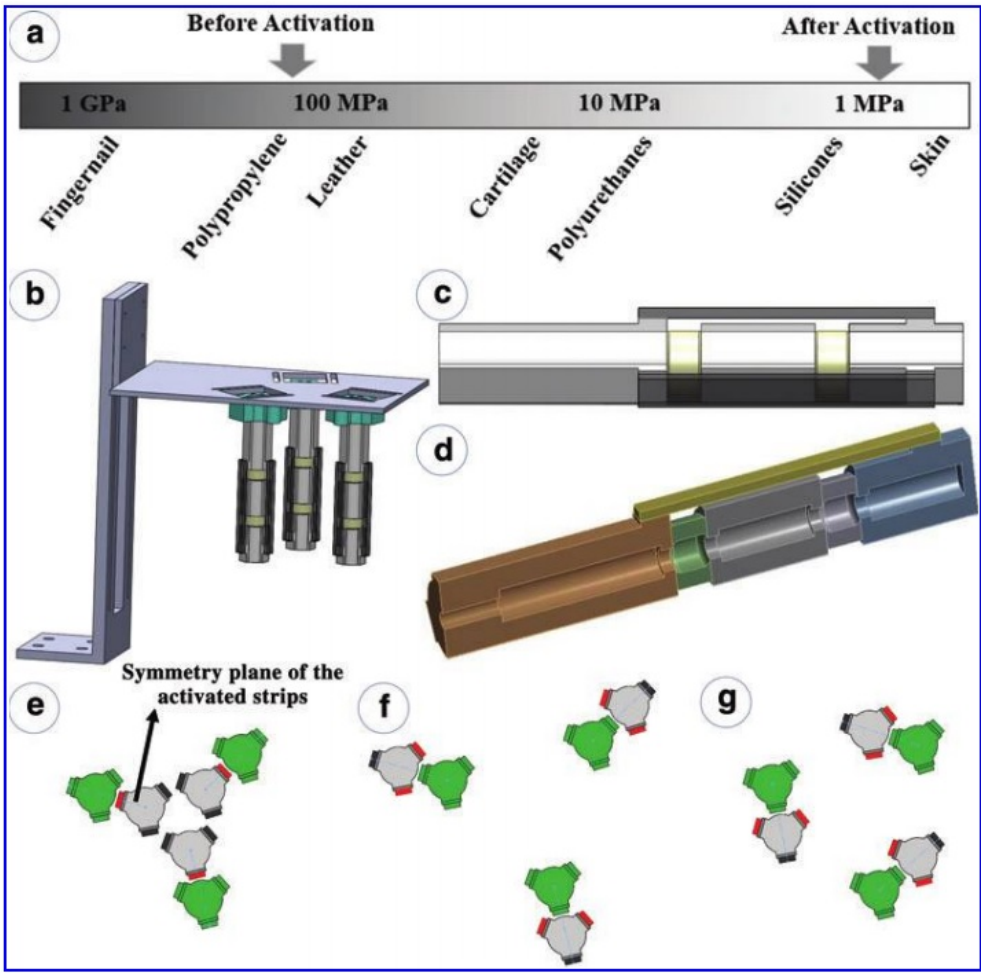

Figure 2.1: Principles of operation for the soft gripper. (a) Range of the tunable rigidity for cPBE. (b)The proposed soft gripper consists of three soft fingers, three finger holders, and two table top metal fixtures. (c) The soft finger consists of three PDMS phalanges, two Ecoflex joints, and three rigidity tunable ligaments. (d) Undeformed crosssectional view of the soft finger. (e) Bottom view of the nonactivated (green)andactivated gripper when the three outer ligaments (red)ofthe fingers are activated and generate a grasping configuration. (f) When the two inner ligaments of each finger are activated, a dropping manipulation is achieved. (g) When the outer and one of the inner ligaments of each finger are activated, a twisting manipulation is achieved.

2.2 Materials

The soft pneumatic finger is made of PDMS phalanges, Ecoflex joints, and cPBE-PDMS rigidity tunable composite ligaments. The PDMS and the Ecoflex joints are made of Sylgard 184 (Dow Corning, Inc.) and Ecoflex 0050 (Smooth-on, Inc.), respectively. Both segments are produced with elastomer casting using 3D printed molds (Objet 24; Stratasys, Ltd.).

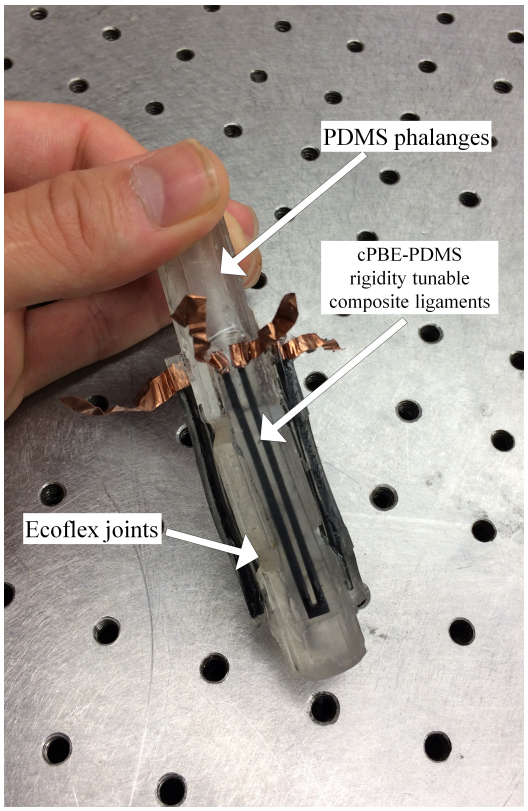

Figure 2.2: Each soft gripper finger consists of three PDMS phalanges, two Ecoflex joints, and three cPBE-PDMS ligaments.

2.2.1 cPBE-PDMS Ligaments

The cPBE was produced by blending a propylene/ethylene copolymer with a percolating network of structured carbon black. It has a weight composition of 51/9/40 percent propylene, ethylene and structured carbon black. Custom-ordered pellets are supplied by THEMIX Plastics, Inc (Lake Mills, WI) and pressed between steel plates at 90 °C to form thin sheets [11]. The Figure 2.3 shows the manufacturing process of U-shaped cPBE strips.

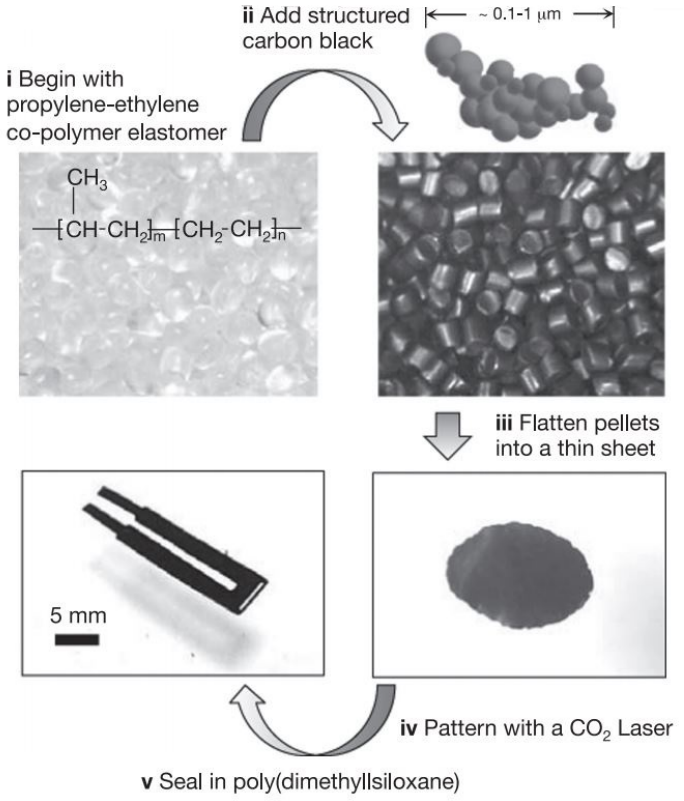

Figure 2.3: Fabrication of cPBE-PDMS composite: (i)–(ii) clear pellets are mixed with structured carbon black to produce cPBE (iii)–(v) When flattened with heat and pressure into thin sheets, the cPBE sheet is patterned with a CO_2 laser [11].

Then, the flattened sheets of cPBE are patterned with a CO_2 laser to form U shaped

strips. After some trial and error, the optimum power and speed of laser was picked to make sure it cuts through the cPBE, but it does not burn the carbon.

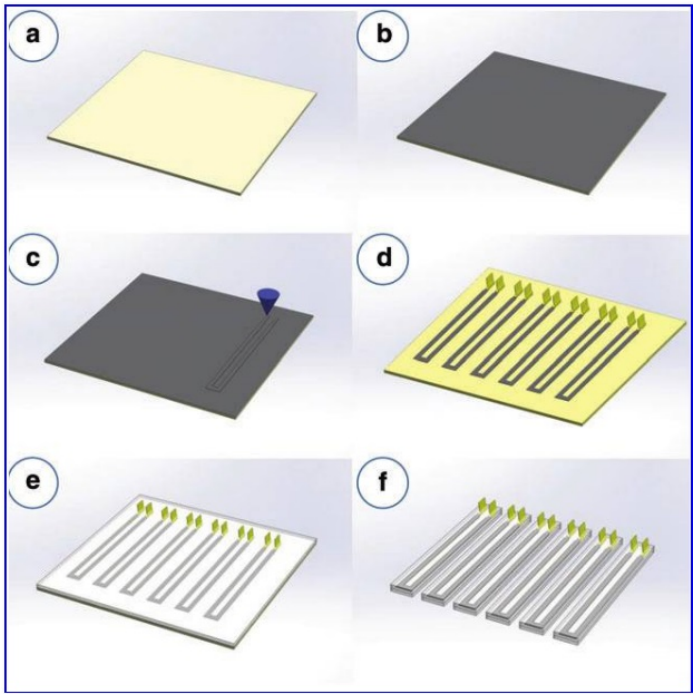

Figure 2.4: Fabrication steps for rigidity tunable strips made of cPBE. (a) Start with a flat smooth metal substrate.(b) Cover with a layer of cPBE. (c) Pattern with a CO_2 laser. (d) Remove the excess cPBE, attach thin strips of copper shim to the terminals, and attach the strips with double-sided tape (VHB, 3M, Inc.) to the substrate. (e) Embed with uncured PDMS and then cure PDMS. (f) Cut edges and release [11].

With the cPBE ends wrapped by thin copper shim wires (Figures 2.5 a and b), the U-shaped cPBE strips were attached onto the bottom of a Petri dish using small pieces of double-sided tape (VHB, 3M, Inc.) such that the cPBE strips were 0.4 mm above the bottom surface of the Petri dish. Then, uncured PDMS solution was poured into the Petri dish to submerge the cPBE strips such that PDMS can embed the cPBE right at halfway of its depth. Next, the composite was cured in a vacuum oven (Across International, Inc.) for 1.5 h at 80°C. Finally, cPBE-PDMS composite strips were carved out of the cured sheet.

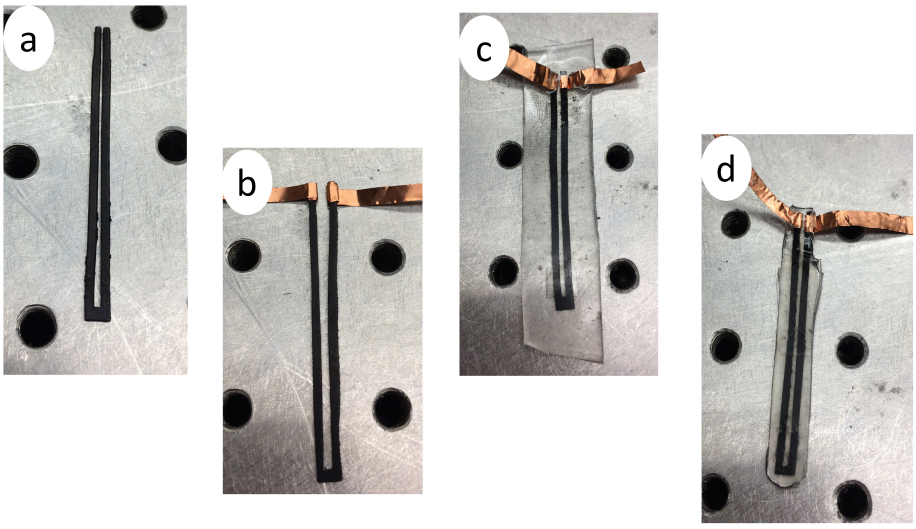

Figure 2.5: Fabrication steps for cPBE-PDMS composite. (1) Start with a flat smooth U-shape strip of cPBE. (2) Wrap the cPBE ends with thin copper shim wires. (3) The cPBE strip is embedded with PDMS. (4) The excess PDMS cut to shape the cPBE-PDMS composite.

The cPBE can rapidly and reversibly change its mechanical rigidity. As mentioned in Chapter 1, the elastomer is rigid in its natural state, but softens when electrically activated. Shown in [11], the tensile modulus changes between 37 and 1.5 MPa for the cPBE-PDMS composite.

It takes 6 s to soften the cPBE-PDMS strip when a 100 V voltage is applied across the two ends of the cPBE film. Using this composite as ligaments on the gripper's fingers significantly reduces the use of external bulky hardware such as pneumatic pumps or valves. It is also rapid, cheap, and easy to fabricate.

2.2.2 PDMS Phalanges and Ecoflex Joints

The PDMS phalanges and Ecoflex joints were designed to have female and male surface features that can fit with each other. This mating is a half circle round edge and is intended to increase the bonding between different materials during assembly. For each of the phalanges (or joints), a mold was designed in SOLIDWORKS and fabricated with a 3D printer. Each mold is a lego-shape structure to make it easier to release cured PDMS and allow for repeated use. Then, the uncured PDMS (or Ecoflex), which is liquid, was poured into the molds and heated up to cure at 90 °C (or at the room temperature for the Ecoflex) for 40 min.

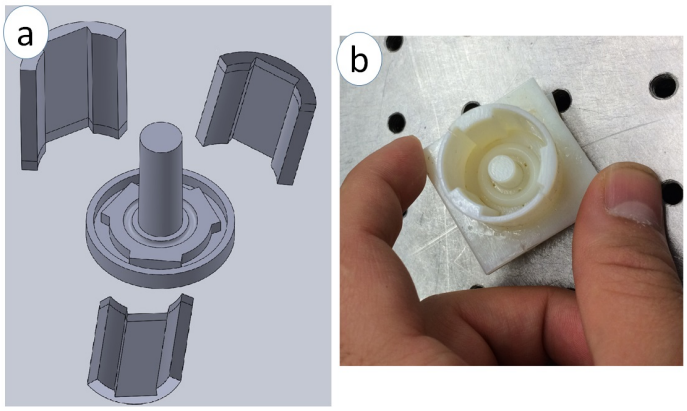

Figure 2.6: The molds for phalanges were designed in SOLIDWORKS and sent to a 3D-printer for fabrication.

The PDMS was supplied as two-part liquid component kits. When mixing the two components, tiny bubbles were present in the mixture. Using THINKY Centrifugal Mixer, the two components were mixed automatically and tiny bubbles were vacuumed out. Since the existence of bubbles limits the efficiency of the parts (phalanges), a vacuum pump connected to the oven vacuumed out the bubble for the second time to make sure no bubble remained in the mixture. Then the mixture was poured to the mold and heated up at 90 °C

for 40 min to cure the PDMS.

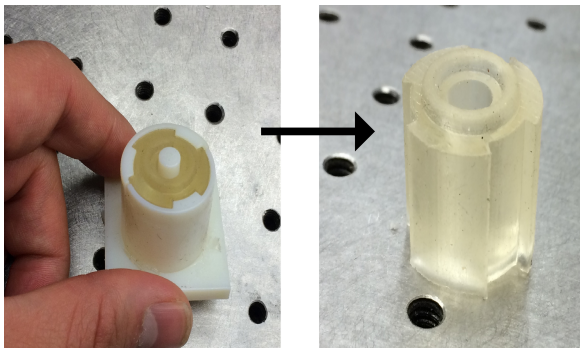

Figure 2.7: The PDMS phalanges cured at 90 °C for 40 min in 3D-printed mold

The same process was implemented to fabricate the joints, but with a softer material, Ecoflex. Ecoflex rubbers are platinum-catalyzed silicones. Two components of Ecoflex were mixed 1A:1B by weight and cured at room temperature for 40 min.

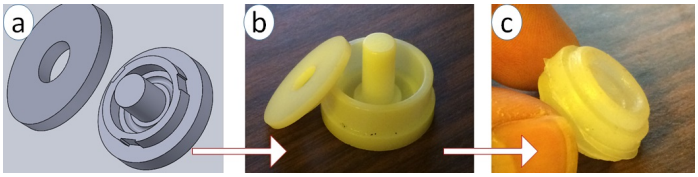

Figure 2.8: (a) The mold for joints was designed in SOLIDWORKS. (b) The mold was fabricated with a 3D printer. (c) The Ecoflex was poured in 3D-printed mold and cured at the room temperature.

2.3 Dimension of the Fingers

As shown in Figure 2.9, the total length of the soft finger is 92 mm including three phalanges and two joints. In another design, the lower phalange, which an object is picked up with, was designed longer to improve the efficiency of the gripper.

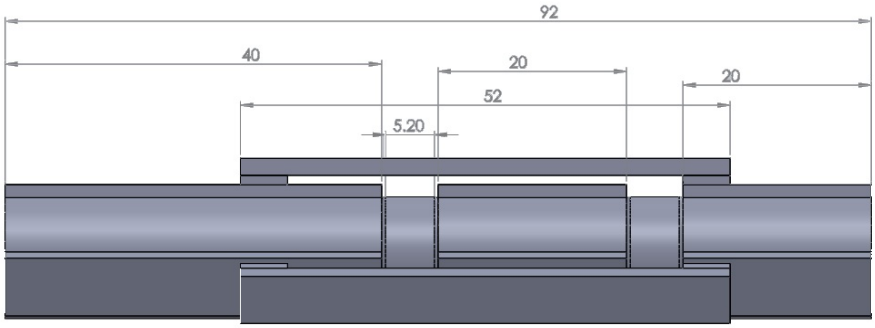

Figure 2.9: The schematic front view of the finger (Unit: mm).

The side view of the gripper is shown in Figure 2.10. The finger has an outer diameter of 13.8 mm and an inner diameter of 6 mm for the hollow inner part. At the top of the finger there is also a hole with a 3 mm diameter to insert an air tube for pressure control.

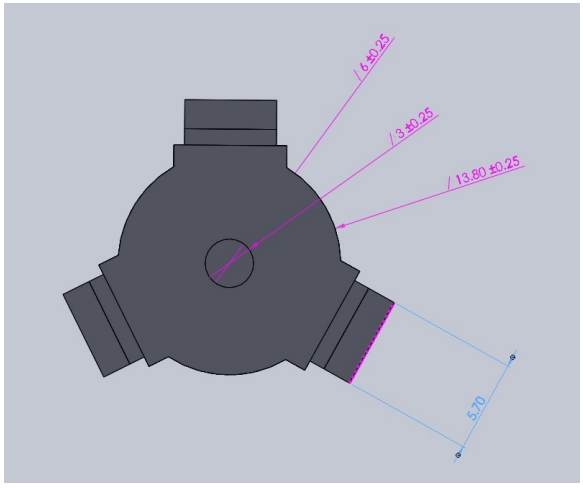

Figure 2.10: The schematic side view of the finger.

As shown in Figure 2.11, the Exoflex joints are thiner than the rest of finger (the outer diameter of the Ecoflex joints is 12 mm, while the outer diameter of the finger is 13.8 mm). This is because Exoflex joints have higher radial expansion than PDMS phalanges when

they are pressurized if they have the same dimensions. To avoid contact between Ecoflex joints and the ligaments, the size of the joints is reduced.

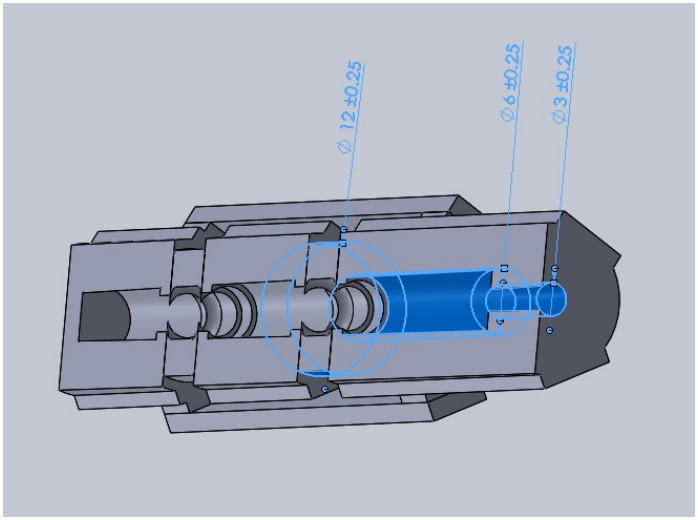

Figure 2.11: The schematic cross-sectional view of the finger.

2.4 Assembly of the Gripper

Each finger assembly needs two Ecoflex joins to attached three PDMS phalanges. Then three cPBE-PDMS ligaments are attached to the side of the finger. The uncured PDMS was used as a glue to stick all components of the finger. Only two parts were attached together in each step. When attaching a joint to phalanges, uncured PDMS was applied to the end surface of the phalange and then the joint was placed on top of that. The whole structure then was cured in the oven for 40 min at 90 °C. To avoid flowing of uncured PDMS onto the joint side wall during curing in the oven, which could affect the finger's functionality, the PDMS segment was always kept on the bottom, underneath the Ecoflex joint. After assembling all the phalanges and joints, the finger was connected to external air pressure to make sure that finger does not have leakage. In the case of leakage, the

connection between Ecoflex joints and PDMS phalanges should be repaired.

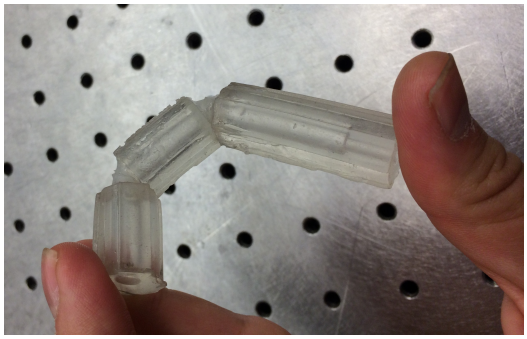

Figure 2.12: The PDMS phalanges and Ecoflex joints were attached with uncured PDMS and tested for functionality before attaching cPBE-PDMS ligaments.

After assembling all the phalanges and joints and making sure that the finger has no leakage when connected to high pressure air, cPBE-PDMS strips were attached onto the sidewall of the phalanges and cured one by one. To avoid flowing of the PDMS in the assembly process, a mixture of half-cured and uncured PDMS as bonding agent was used.

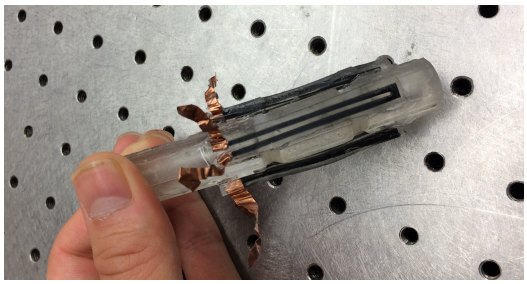

Figure 2.13: Three cPBE-PDMS ligaments were attached to the side wall of the finger.

Finally, a soft latex rubber tube (McMaster-Carr, Inc.) was inserted into a small hole in one end of the finger and sealed with uncured PDMS. This tube was connected to the air pressure regulator for activation and deactivation of the soft gripper.

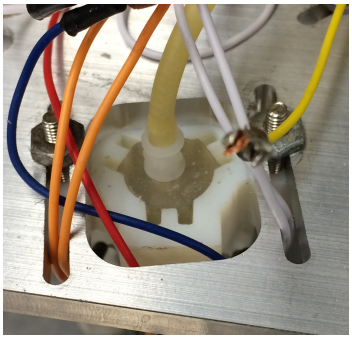

Figure 2.14: The high pressure air tube was attached to the finger and sealed with PDMS.

As shown in Figure 2.15, three fingers were inserted into three 3D-printed finger holders, which were bolted to the rails on an L-shaped metallic fixture to form a gripper. The opening between the fingers and the vertical position of the gripper can be manually adjusted. Next, the copper leads of the fingers' ligaments were connected to an electrical board, where electrical circuits and switches can be designed to selectively activate any combination of the nine ligaments (strips). The electrical board was connected to an electrical power supply (GPR-30H10D; GW Instek, Inc.), which can be used to activate selected ligaments. Finally, the three rubber tubes coming out of the fingers' chambers were connected to a single air pressure regulator (PneumaticPlus, Inc.), which was connected to a source of high-pressure air in the laboratory.

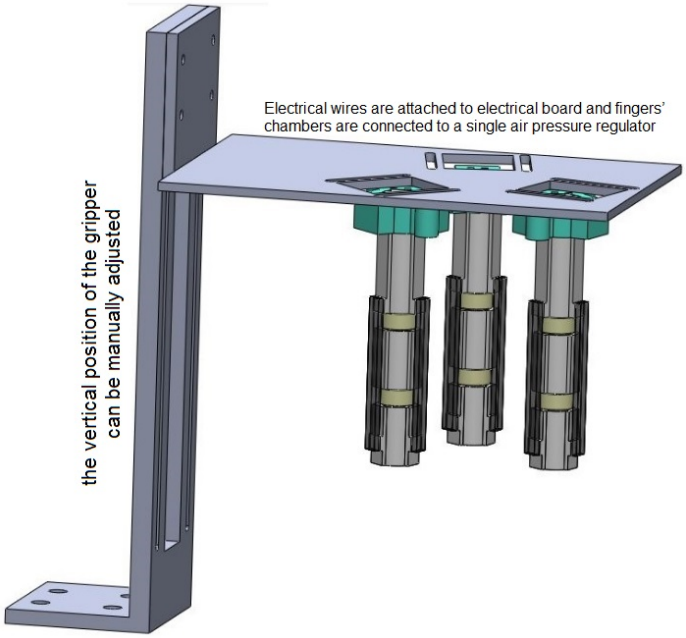

Figure 2.15: The schematic of the soft gripper with three fingers attached to an L-shaped fixture.

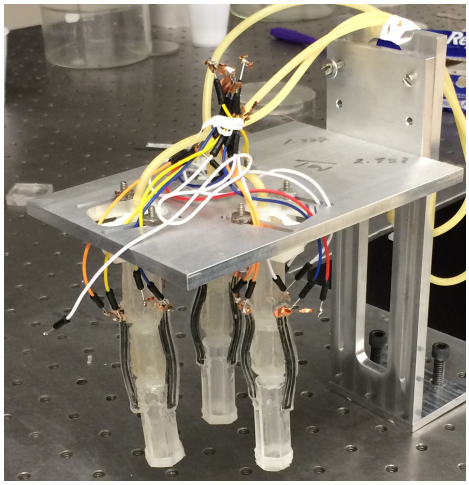

Figure 2.16: Experimental realization of the soft gripper with three fingers attached to an L-shaped fixture.

Chapter 3

Mechanical Tests

3.1 Mechanical Behavior of the Soft Finger

To characterize the effective force and deflection of the fingertip under different air pressure inputs, a soft finger was mounted horizontally using the aforementioned fixtures on the table such that one of the ligaments was positioned horizontally on the top, parallel to the table surface (Figure 3.1).

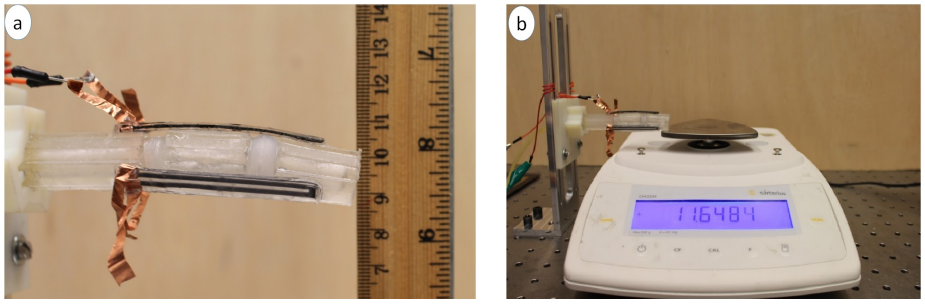

Figure 3.1: (a) Mechanical testing setup for individual soft finger fingertip deflection measurements. (b) Mechanical testing setup for individual soft finger bending force measurements.

3.1.1 Fingertip Deflections

To measure the fingertip deflections under different air pressure inputs, the top ligament was activated, the supporting fixture was removed, and then the gauge pressure was increased from 0 to 70 kPa in 10 kPa increments. The deflections were recorded at each increment with a vertical ruler (Figure 3.1 a). Due to the self-weight of the finger, in both force and deflection measurements, there will be an initial value when the gauge pressure is zero.

3.1.2 Fingertip Bending Forces

A supporting horizontal fixture was used to make sure that at the beginning of the tests the finger was at a horizontal position. To measure the bending force at the fingertip after activation of the finger, a digital scale (CPA224S; Sartorius, Inc.) was positioned under the fingertip such that the scale pan barely touched the fingertip before removing the supporting horizontal fixture. To simulate the frictionless support at the interface of the scale pan and the fingertip, olive oil was applied on the surface of the scale pan. Finally, the top ligament was activated, the supporting fixture was removed, and the gauge pressure was increased from 0 to 70 kPa in 10 kPa increments to measure the effective forces at different air pressure inputs, as shown in Figure3.1 b.

3.2 Mechanical Characterization of Elastomers

A Young's modulus value of 1.04 MPa was reported in Shan et al. [11] for cured PDMS. However, in this study, PDMS phalanges were cured in the oven several times (about 5 h in

total at 90 °C) during the process of assembling different components. Therefore, a series of tensile tests were independently performed on homogeneous PDMS specimens cured multiple times in the oven. The Young's modulus is found to be $E_{PDMS} = 4.12 - 0.20$ MPa based on testing of four samples, which is about 4X higher than the reported values in other literatures [11].

Due to the large deformation regime encountered in the finger joints during their functioning, the nonlinear hyperelastic neo-Hookean model is used to capture the stress/strain behavior of the Ecoflex parts. Tensile tests were performed on homogeneous oven-cured Ecoflex samples. Using the relationships in Equations 3.1, 3.2 and 3.3, the initial shear modulus μ_{Eco} is found to be 0.0638 ± 0.00637 MPa based on testing of three samples. The incompressibility parameter d thus found to be 0.00626 $(\text{MPa})^{-1}$ using a Poisson ratio $\nu_{Eco} = 0.499$. Here in the equations, σ is the stress, λ is the stretch, ϵ is the strain, and κ is the bulk modulus:

$$\sigma = \mu(\lambda^2 - 1/\lambda) \tag{3.1}$$

$$\lambda = 1 + \epsilon \tag{3.2}$$

$$\kappa = 2/d = \mu/(1 - 2\nu) \tag{3.3}$$

Chapter 4

Modeling, Results and Discussions

4.1 Finite Element Analysis

To better understand the mechanical behavior of the proposed finger, simulations of FEA were conducted with the commercial FEA package ANSYS. A 3D model of the finger with the real finger dimensions was used to simulate the stress/strain distribution during functioning as well as the deflection and reaction force at the fingertip. Due to the twofold symmetry of the finger geometry, only a half of the finger was modeled. A fixed support boundary condition was applied at the base of the finger and the fingertip was free to move. Air pressure was applied inside the finger chamber normal to the chamber surfaces. Frictionless support boundary condition was implemented on the symmetry plane of the finger. Frictionless contacts were defined between the contacting surfaces of the ligaments and the finger phalanges such that the ligaments can freely slide on the finger without penetration. The finger model was reproduced using PDMS, Ecoflex, and cPBE-PDMS composite properties for finger phalanges, joints, and ligaments, respectively. Isotropic, homogeneous, and

linear elastic properties were assigned to the finger phalanges and ligaments due to small strain regime. Poisson's ratio of the PDMS was set to be 0.499 and its Young's modulus was set to be E_PDMS = 4.12 MPa as measured. The cPBE-PDMS composite strips were treated as a homogenous material with a Young's modulus of 30.12 MPa before activation, and 0.86 MPa after activation, calculated using methods and data from Shan et al. [11].

Taking the self-weight of the finger into account, the model was run for two scenarios corresponding to the mechanical characterization testing conducted for individual fingers: (1) there was a horizontal frictionless support at the fingertip with no vertical deflection allowed, to find the effective bending force of the fingertip at various pressure inputs and (2) there was no constraint on displacement of the fingertip, to compute the deflection of the fingertip at various pressure inputs.

The deflections at the fingertip under increasing air pressure inputs predicted by the FEA and measured in the experiments are compared in Figure 4.1 a. As shown, the computational predictions agree well with the experimental results. A 1.93 mm initial deflection due to self-weight at the fingertip was predicted by the FEA and verified by the experiment before applying the pressure. The fingertip deflection at p = 70 kPa predicted by FEA is 8.29 mm, whereas the measured value is 9.60 mm, which is a 15.8% difference based on the FEA results. The experiment was stopped at 70 kPa because for higher pressure, leaking from the interface between the joints and the phalanges might happen. What is more, the slope of the curve increases with increasing air pressure, which suggests that improving the interfacial strength between the joints and the phalanges will enable larger deflections.

Figure 4.2 shows the experimental and modeling results of the fingertip bending force when the fingertip was not allowed to move in the vertical direction. As observed, the body of the finger moved upward due to constraint applied at the fingertip. The maximum strain and stress predicted by the FEA at p = 70 kPa are 88% on the inner surface of the

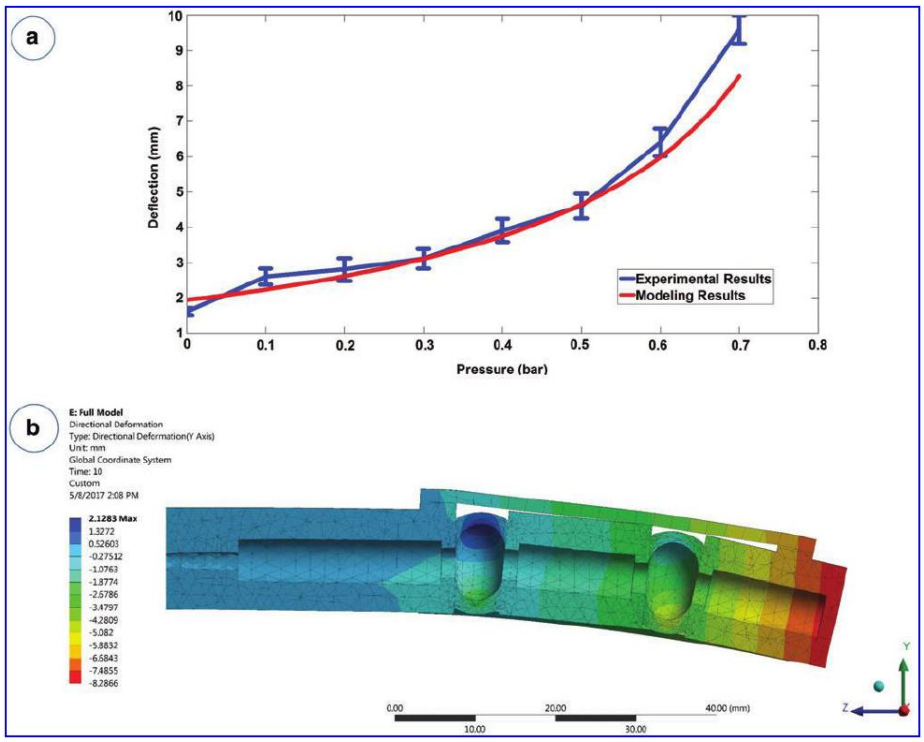

Figure 4.1: (a) Comparison between the experimental and modeling results of fingertip deflections versus different air pressure inputs; the error bars are all based on three tests and the deflection direction is downward. (b) Deformed half finger when the input air pressure is 70 kPa showing the displacement distribution of the finger body.

second joint and 0.66 MPa at the attaching point of the strips to the body, respectively. The highest deflection is also seen on the inner surface of the second joint to be 4.29 mm, which is expected due to the fixed support at the finger base and the frictionless support on the fingertip in the horizontal plane. Comparing the experimental and modeling results, the maximum difference is found to be 11.5% when the input air pressure is p = 30 kPa. Similar to the deflection plot in Figure 5, the bending force at the fingertip increases non-linearly as the pressure inside the finger chamber increased. So once again, it implies that improving the interfacial strength between the joints and the phalanges becomes critical in achieving higher gripping forces.

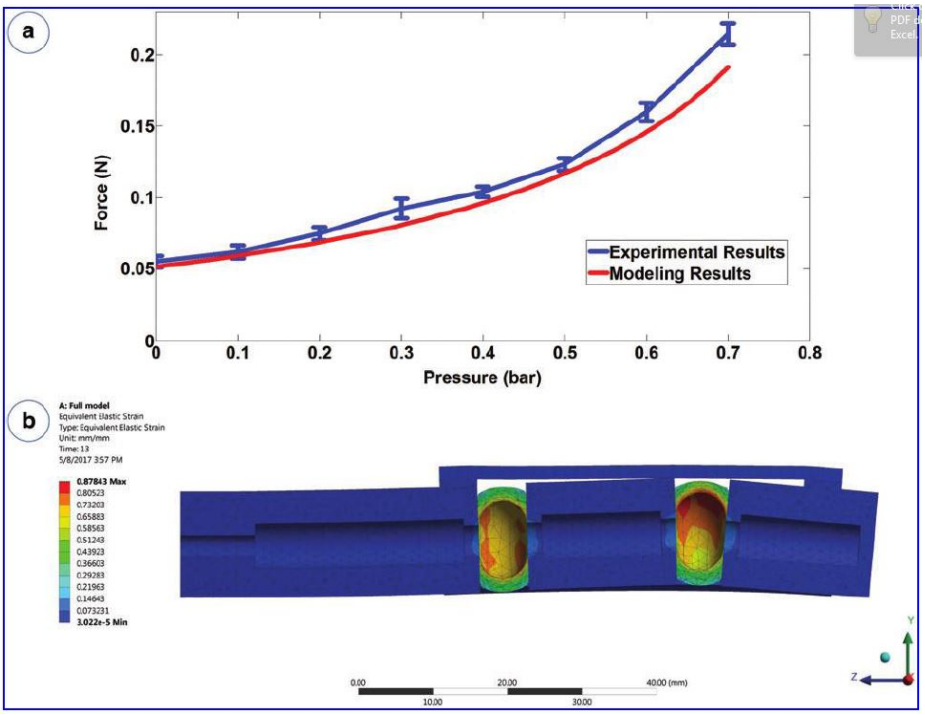

Figure 4.2: (a) Comparison between the experimental and modeling results of fingertip bending forces versus different air pressure inputs; the error bars are all based on three tests. (b) Deformed half finger when the input air pressure is 70 kPa showing the strain distribution of the finger body.

4.2 Manipulation of Objects with Different Shapes

To better understand the working principle of the soft gripper and its efficiency to pick up objects with different shapes, we have picked up different objects shown in Figure 4.3. Note that two different sizes (longer and shorter) of the phalanges were used based on the shape and weight of the objects. A simple electrical circuit was used to control the activation sequences of the strips, with two switches designated for activating grasping and twisting, respectively.

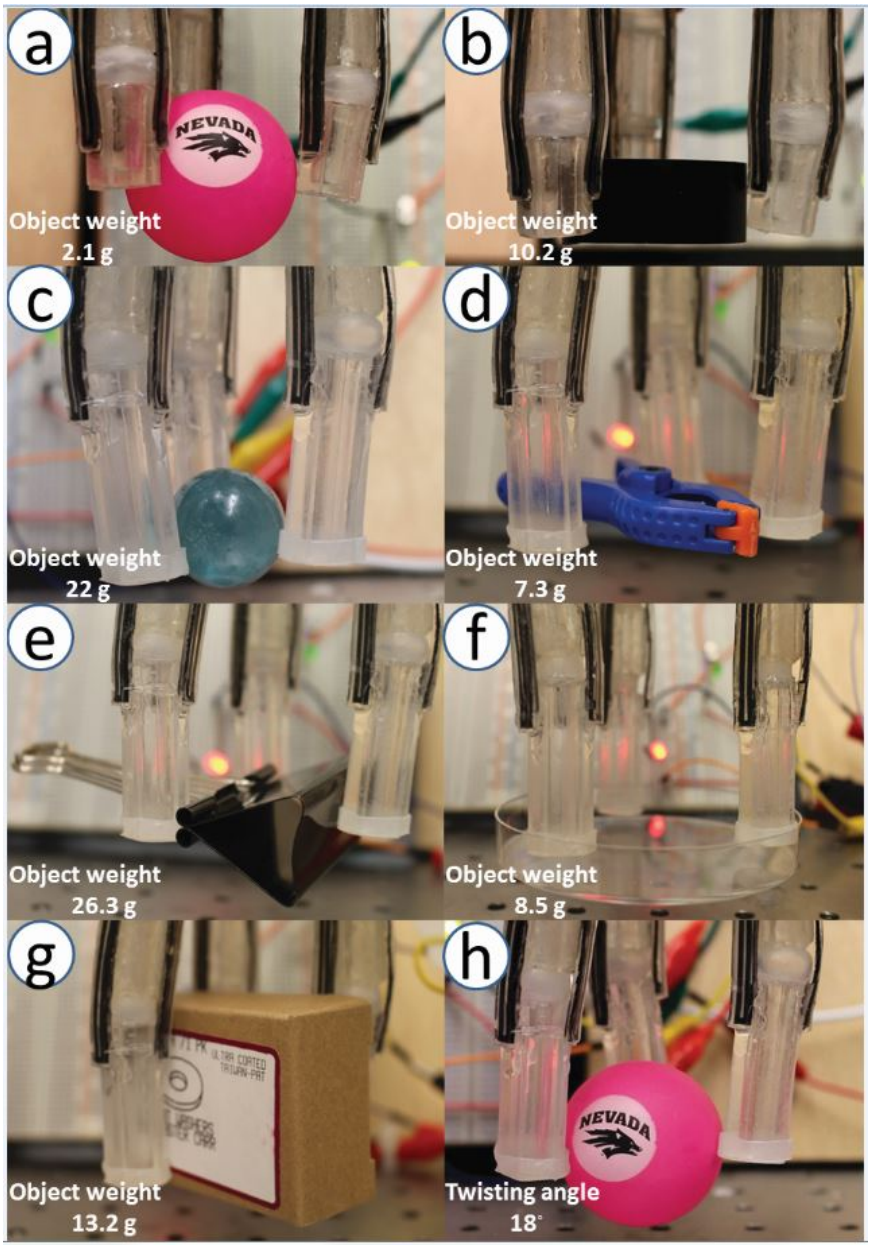

Figure 4.3: Grasping, releasing, and twisting manipulations by two soft grippers (a) Grasping of a 2.1 g ping-pong ball. (b) Grasping of a 10.2 g tape roll. (c) Grasping of a 22.0 g glass ball. (d) Grasping of a 7.3 g plastic nylon spring clamp. (e) Grasping of a 26.3 g paper clip. (f) Grasping of an 8.5 g plastic Petri dish. (g) Grasping of a 13.2 g paper box. (h) Twisting of a 2.1 g ping-pong ball immediately after picking it up.

To achieve grasping, the three outer ligaments of the soft gripper (Figure 4.4 a) were activated at the same time. Figures 4.3 a and b show that the gripper picked up a ping-pong

ball and a roll of tape with ease. The weights of the ping-pong ball and the tape roll are 2.1 g and 10.2 g, respectively. The gripper was not able to pick up a glass ball of 22 g weight due to the lack of friction between the PDMS fingertip surface and the glass surface. To enhance the friction coefficient at the fingertip, an elastomer band (Ecoflex 0050; Smooth-On) was added to the fingertip and the grasping was successful (Figure 4.3 c). We also used the gripper to pick up objects with complicated geometries such as a plastic nylon spring clamp (Figure 4.3 d), a paper clip (Figure 4.3 e), a plastic Petri dish (Figure 4.3 f), and a paper box (Figure 4.3 g). In all cases, the pickup processes were finished within 10 s.

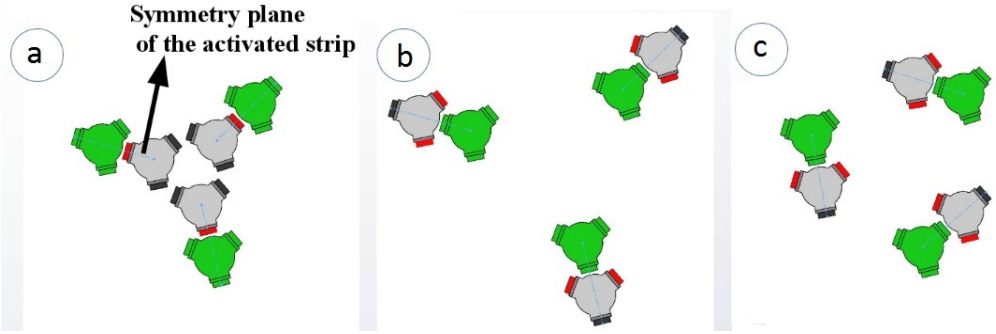

Figure 4.4: (a) Bottom view of the nonactivated (green) and activated gripper when the three outer ligaments (red) of the fingers are activated and generate a grasping configuration. (b) When the two inner ligaments of each finger are activated, a dropping manipulation is achieved. (c) When the outer and one of the inner ligaments of each finger are activated, a twisting manipulation is achieved.

4.3 Object Twisting Manipulation

Object twisting manipulation has seldom been shown in recent soft gripper designs, with previous demonstrations relying on multiple pneumatic chambers within each finger. In our study, twisting manipulation begins by first grasping the object with a finger closing motion. Then, while the object is being held, another set of ligaments of the fingers, as shown in

Figure 4.4 c, is activated to generate the twisting motion. Here the gripper composed of soft fingers with longer distal phalanges is used to twist a ping-pong ball immediately after picking it up (Figure 4.3 a). Figure 4.5 shows a series of images of the twisted ping-pong ball, together with the plot of twisting angle versus time. After activating the second ligament of each finger to rotate the ball, the effective force of the fingertip holding the ball is observed to be decreased. However, as the effective force of the fingertip in the gripping configuration is still higher than the required force to hold the ball, the twisting manipulation can be successfully completed. As we see from Figure 4.5, the twisting process was almost done in 15 s. And a twisting angle about 18° was achieved using the current version of the fingers. More twisting could be achieved by optimizing the geometry of the fingers.

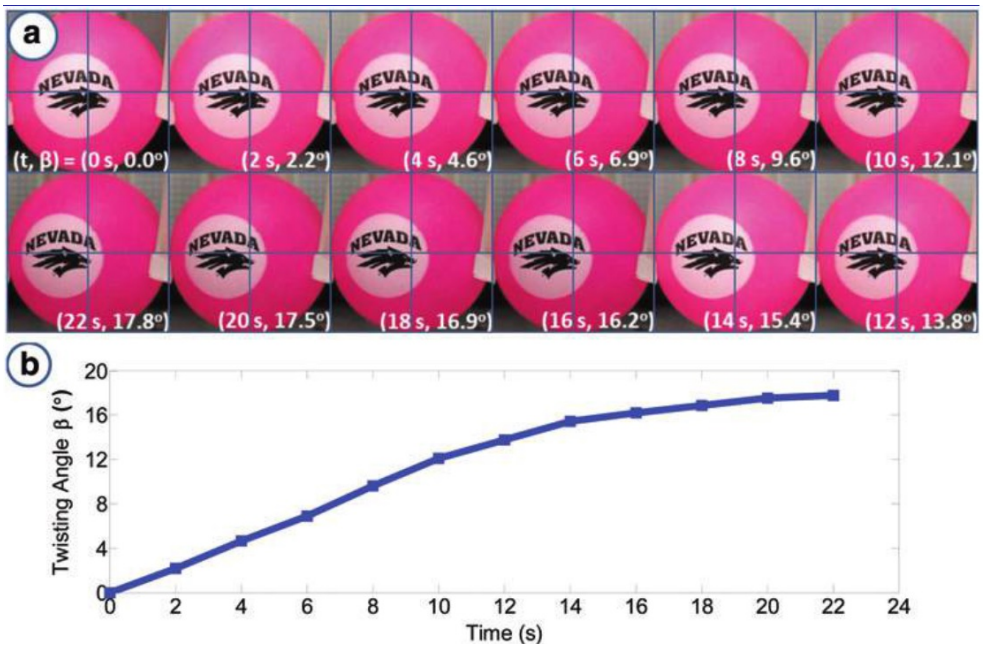

Figure 4.5: (a) Series of snapshots of twisting of a 2.1 g ping-pong ball. (b) Twisting angles versus activation time plot indicates that the twisting manipulation can be finished in roughly 15 s.

Chapter 5

Conclusions, Future Work and Perspectives

In this study, we design a universal soft gripper utilizing rigidity tunable elastomer as ligaments for its three fingers. A single central source of pressure is used to control the air pressure inside the finger chambers, which greatly reduces the complexity of supporting hardware when generating complicated manipulations. We also conducted mechanical testing and finite element molding to better understand the mechanical behavior of single soft fingers.

Each tunable stiffness ligament is a composite of PDMS embedded with cPBE strips. The composite rigidity reversibly changes when it is heated up by Joule heating through cPBE strips. Once one of the ligaments is activated, the pressurized finger is bent to the opposite direction of the activated ligament due to the geometrical asymmetry. The soft gripper is able to manipulate objects with different shapes and sizes by activating different

combinations of ligaments.

We have demonstrated that this soft gripper can grasp and release various objects in seconds. This kind of soft gripper can potentially handle objects in narrow channels and holes the same way as human fingers. More importantly, in this design, not only can all the fingers be individually controlled but they can also be actively tuned for functionality after being fabricated thanks to the rigidity tunable ligaments. This enables the soft gripper to perform closing, twisting, and opening motions previously demonstrated by multichamber pneumatic grippers using only a single internal air pressure.

There is of course room for improvement for the design of soft grippers. For one, the dynamic control of the soft gripper hinges on the activation of the rigidity tunable ligaments, which is controlled by Joule heating, a slow process in nature. Faster activation time can be achieved either by designing a new rigidity tunable material that can be activated with Joule heating much faster (less than one second), or by switching to alternative rigidity tuning mechanisms other than Joule heating, such as magnetism, dielectric effects, etc.

This study has been conducted under the rising interests in soft robotics, flexible electronics and compliant wearable/medical devices, which is concurrent with the surging of artificial intelligence facilitated by big data analytics. Combining the innovations in both hardware and software, the human kind will soon witness the new era of intelligent machines. I hope that this work has contributed a tiny bit to this technological revolution.

Bibliography

[1] Ruben D Ponce Wong, Jonathan D Posner, and Veronica J Santos. Flexible microfluidic normal force sensor skin for tactile feedback. *Sensors and Actuators A: Physical*, 179:62–69, 2012.

[2] Peter Roberts, Dana D Damian, Wanliang Shan, Tong Lu, and Carmel Majidi. Soft-matter capacitive sensor for measuring shear and pressure deformation. In *Robotics and Automation (ICRA), 2013 IEEE International Conference on*, pages 3529–3534. IEEE, 2013.

[3] Martin Weigel, Tong Lu, Gilles Bailly, Antti Oulasvirta, Carmel Majidi, and Jürgen Steimle. iskin: Flexible, stretchable and visually customizable on-body touch sensors for mobile computing. In *Proceedings of the 33rd Annual ACM Conference on Human Factors in Computing Systems*, pages 2991–3000. ACM, 2015.

[4] Tong Lu, Lauren Finkenauer, James Wissman, and Carmel Majidi. Rapid prototyping for soft-matter electronics. *Advanced Functional Materials*, 24(22):3351–3356, 2014.

[5] Minwoo Park, Jaeyoon Park, and Unyong Jeong. Design of conductive composite elastomers for stretchable electronics. *Nano Today*, 9(2):244–260, 2014.

[6] Seung Hee Jeong, Klas Hjort, and Zhigang Wu. Tape transfer printing of a liquid metal alloy for stretchable rf electronics. *Sensors*, 14(9):16311–16321, 2014.

[7] Jifei Ou, Lining Yao, Daniel Tauber, Jürgen Steimle, Ryuma Niiyama, and Hiroshi Ishii. jamsheets: thin interfaces with tunable stiffness enabled by layer jamming. In *Proceedings of the 8th International Conference on Tangible, Embedded and Embodied Interaction*, pages 65–72. ACM, 2014.

[8] Farhan Gandhi and Sang-Guk Kang. Beams with controllable flexural stiffness. In *The 14th International Symposium on: Smart Structures and Materials & Nondestructive Evaluation and Health Monitoring*, pages 65251I–65251I. International Society for Optics and Photonics, 2007.

[9] MA McEvoy and Nikolaus Correll. Shape change through programmable stiffness. In *International Symposium on Experimental Robotics (ISER), Marrakech, Morocco*, 2014.

[10] Wanliang Shan, Tong Lu, and Carmel Majidi. Soft-matter composites with electrically tunable elastic rigidity. *Smart Materials and Structures*, 22(8):085005, 2013.

[11] Wanliang Shan, Stuart Diller, Abbas Tutcuoglu, and Carmel Majidi. Rigidity-tuning conductive elastomer. *Smart Materials and Structures*, 24(6):065001, 2015.

[12] Bryan E Schubert and Dario Floreano. Variable stiffness material based on rigid low-melting-point-alloy microstructures embedded in soft poly (dimethylsiloxane)(pdms). *Rsc Advances*, 3(46):24671–24679, 2013.

[13] Thomas P Chenal, Jennifer C Case, Jamie Paik, and Rebecca K Kramer. Variable stiffness fabrics with embedded shape memory materials for wearable applications. In *Intelligent Robots and Systems (IROS 2014), 2014 IEEE/RSJ International Conference on*, pages 2827–2831. IEEE, 2014.

[14] Takashi Yoshimi, Naoyuki Iwata, Makoto Mizukawa, and Yoshinobu Ando. Picking up operation of thin objects by robot arm with two-fingered parallel soft gripper. In *Advanced Robotics and its Social Impacts (ARSO), 2012 IEEE Workshop on*, pages 7–12. IEEE, 2012.

[15] Eric Brown, Nicholas Rodenberg, John Amend, Annan Mozeika, Erik Steltz, Mitchell R Zakin, Hod Lipson, and Heinrich M Jaeger. Universal robotic gripper based on the jamming of granular material. *Proceedings of the National Academy of Sciences*, 107(44):18809–18814, 2010.

[16] Maria Elena Giannaccini, Ian Georgilas, Ian Horsfield, BHPM Peiris, Alexander Lenz, Anthony G Pipe, and Sanja Dogramadzi. A variable compliance, soft gripper. *Autonomous Robots*, 36(1-2):93–107, 2014.

[17] Oluwaseun Araromi, Irina Gavrilovich, Jun Shintake, Samuel Rosset, Martin Richard, Volker Gass, Herbert R Shea, et al. Rollable multisegment dielectric elastomer minimum energy structures for a deployable microsatellite gripper. *Mechatronics, IEEE/ASME Transactions on*, 20(1):438–446, 2015.

[18] Amir Firouzeh, Seyed Sina Mirrazavi Salehian, Aude Billard, and Jamie Paik. An under actuated robotic arm with adjustable stiffness shape memory polymer joints.

[19] Carmel Majidi. Soft robotics: a perspective—current trends and prospects for the future. *Soft Robotics*, 1(1):5–11, 2014.

[20] Nicholas W Bartlett, Michael T Tolley, Johannes TB Overvelde, James C Weaver, Bobak Mosadegh, Katia Bertoldi, George M Whitesides, and Robert J Wood. A 3d-printed, functionally graded soft robot powered by combustion. *Science*, 349(6244):161–165, 2015.

[21] Yong-Lae Park, Carmel Majidi, Rebecca Kramer, Phillipe Bérard, and Robert J Wood. Hyperelastic pressure sensing with a liquid-embedded elastomer. *Journal of Micromechanics and Microengineering*, 20(12):125029, 2010.

[22] Mallory L Hammock, Alex Chortos, Benjamin C-K Tee, Jeffrey B-H Tok, and Zhenan Bao. 25th anniversary article: The evolution of electronic skin (e-skin): A brief history, design considerations, and recent progress. *Advanced Materials*, 25(42):5997–6038, 2013.

[23] Vladimir Lumelsky, Michael S Shur, and Sigurd Wagner. *Sensitive skin*. World Scientific, 2000.

[24] Takao Someya, Tsuyoshi Sekitani, Shingo Iba, Yusaku Kato, Hiroshi Kawaguchi, and Takayasu Sakurai. A large-area, flexible pressure sensor matrix with organic field-effect transistors for artificial skin applications. *Proceedings of the National Academy of Sciences of the United States of America*, 101(27):9966–9970, 2004.

[25] Hyun-Joong Kim, Chulwoo Son, and Babak Ziaie. A multiaxial stretchable interconnect using liquid-alloy-filled elastomeric microchannels. *Applied Physics Letters*, 92(1):011904, 2008.

[26] Shi Cheng and Zhigang Wu. A microfluidic, reversibly stretchable, large-area wireless strain sensor. *Advanced Functional Materials*, 21(12):2282–2290, 2011.

[27] Sandesh S Deshmukh, Sreepriya Vedantam, Jyeshtharaj B Joshi, and Sudhir B Koganti. Computational flow modeling and visualization in the annular region of annular centrifugal extractor. *Industrial & Engineering Chemistry Research*, 46(25):8343–8354, 2007.

[28] Arjo Loeve, Paul Breedveld, and Jenny Dankelman. Scopes too flexible... and too stiff. *IEEE pulse*, 1(3):26–41, 2010.

[29] C Thill, J Etches, I Bond, K Potter, and P Weaver. Morphing skins. *The Aeronautical Journal*, 112(1129):117–139, 2008.

[30] L Janke, C Czaderski, M Motavalli, and J Ruth. Applications of shape memory alloys in civil engineering structures—overview, limits and new ideas. *Materials and Structures*, 38(5):578–592, 2005.

[31] Hiroyuki Nakai, Yasuo Kuniyoshi, Masayuki Inaba, and Hirochika Inoue. Metamorphic robot made of low melting point alloy. In *Intelligent Robots and Systems, 2002. IEEE/RSJ International Conference on*, volume 2, pages 2025–2030. IEEE, 2002.

[32] A Bergamini, R Christen, and M Motavalli. Electrostatically tunable bending stiffness in a gfrp–cfrp composite beam. *Smart materials and structures*, 16(3):575, 2007.

[33] Gabriel Murray and Farhan Gandhi. Multi-layered controllable stiffness beams for morphing: energy, actuation force, and material strain considerations. *Smart Materials and Structures*, 19(4):045002, 2010.

[34] J Wissman, L Finkenauer, L Deseri, and C Majidi. Saddle-like deformation in a dielectric elastomer actuator embedded with liquid-phase gallium-indium electrodes. *Journal of Applied Physics*, 116(14):144905, 2014.

[35] WL Shan, T Lu, ZH Wang, and C Majidi. Thermal analysis and design of a multilayered rigidity tunable composite. *International Journal of Heat and Mass Transfer*, 66:271–278, 2013.

[36] Deepak Trivedi, Christopher D Rahn, William M Kier, and Ian D Walker. Soft robotics: Biological inspiration, state of the art, and future research. *Applied Bionics and Biomechanics*, 5(3):99–117, 2008.

[37] G Robinson and J Bruce C Davies. Continuum robots-a state of the art. In *Robotics and Automation, 1999. Proceedings. 1999 IEEE International Conference on*, volume 4, pages 2849–2854. IEEE, 1999.

[38] Nabil Simaan, Russell Taylor, and Paul Flint. A dexterous system for laryngeal surgery. In *Robotics and Automation, 2004. Proceedings. ICRA'04. 2004 IEEE International Conference on*, volume 1, pages 351–357. IEEE, 2004.

[39] Ryuta Ozawa, Kazunori Hashirii, and Hiroaki Kobayashi. Design and control of underactuated tendon-driven mechanisms. In *Robotics and Automation, 2009. ICRA'09. IEEE International Conference on*, pages 1522–1527. IEEE, 2009.

[40] Sen W Kwok, Stephen A Morin, Bobak Mosadegh, Ju Hee So, Robert F Shepherd, Ramses V Martinez, Barbara Smith, Felice C Simeone, Adam A Stokes, and

George M Whitesides. Magnetic assembly of soft robots with hard components. *Advanced Functional Materials*, 24(15):2180–2187, 2014.

[41] Samuel Shian, Katia Bertoldi, and David R Clarke. Dielectric elastomer based "grippers" for soft robotics. *Advanced Materials*, 27(43):6814–6819, 2015.

[42] Nadia G Cheng, Maxim B Lobovsky, Steven J Keating, Adam M Setapen, Katy Gero, Anette E Hosoi, Karl D Iagnemma, et al. Design and analysis of a robust, low-cost, highly articulated manipulator enabled by jamming of granular media. In *Robotics and Automation (ICRA), 2012 IEEE International Conference on*, pages 4328–4333. IEEE, 2012.

Appendix I: Journal Publication Based on This Work

This study was conducted under the advising of Dr. Wanliang Shan. The results have been published in a paper entitled “A Soft Gripper with Rigidity Tunable Elastomer Strips as Ligaments” with Soft Robotics, a leading journal in robotics with an impact factor of 8.6 as of 2017. The first two authors, Amir M. Nasab and Amin Sabzehzar, contributed equally to main design, fabrication, modeling and testing of the soft gripper. The first page and the last page of the paper have also been attached here.

SOFT ROBOTICS
Volume 00, Number 00, 2017

DOI: 10.1089/soro.2016.0039

SoRo
Soft Robotics

ORIGINAL ARTICLE

A Soft Gripper with Rigidity Tunable Elastomer Strips as Ligaments

Amir Mohammadi Nasab,[1,*] Amin Sabzehzar,[1,*] Milad Tatari,[1] Carmel Majidi,[2] and Wanliang Shan[1]

Abstract

Like their natural counterparts, soft bioinspired robots capable of actively tuning their mechanical rigidity can rapidly transition between a broad range of motor tasks—from lifting heavy loads to dexterous manipulation of delicate objects. Reversible rigidity tuning also enables soft robot actuators to reroute their internal loading and alter their mode of deformation in response to intrinsic activation. In this study, we demonstrate this principle with a three-fingered pneumatic gripper that contains "programmable" ligaments that change stiffness when activated with electrical current. The ligaments are composed of a conductive, thermoplastic elastomer composite that reversibly softens under resistive heating. Depending on which ligaments are activated, the gripper will bend inward to pick up an object, bend laterally to twist it, and bend outward to release it. All of the gripper motions are generated with a single pneumatic source of pressure. An activation–deactivation cycle can be completed within 15 s. The ability to incorporate electrically programmable ligaments in a pneumatic or hydraulic actuator has the potential to enhance versatility and reduce dependency on tubing and valves.

Keywords: soft gripper, rigidity tunable elastomer, grasping and twisting

Introduction

Natural organisms use striated muscles, catch connective tissues, or muscular hydrostats to alter the mechanical rigidity of their body and limbs.[1–3] Such stiffness tuning functionality is critical in motor tasks such as grasping that rely on reversible transitions between gentle, mechanically passive contact and heavy load bearing. Similarly, bioinspired and soft robotic grasping systems depend on active rigidity tuning to adapt their mode of operation and rapidly transition between different motor tasks. To match the mechanical properties and versatility of natural grippers, such mechanisms should be lightweight and capable of reversibly changing their effective elastic moduli between 0.1–1 MPa and 10–100 MPa, which correspond to the moduli of soft tissues and hard cartilages in humans.[1–4] Moreover, engineering these mechanisms to respond to moderate electrical voltages enables compatibility with conventional electronics and batteries and limits dependency on pneumatics, hydraulics, motors, internal combustion engines, or other typically bulky mechanical hardware.

In this article, we introduce an electrically controlled soft gripper (Fig. 1) consisting of three soft pneumatic fingers with rigidity tunable elastomer strips as ligaments attached on the sidewalls. Resistive heating through the strips can reversibly change the mechanical rigidity of the ligaments. By applying air pressure, pneumatic fingers bend in the opposite direction of the activated softer ligaments. Collectively, the three fingers can achieve not only grasping and releasing manipulations but also twisting. To validate our experimental results, we also perform finite element analysis (FEA) on a 3D model of the finger to predict the grasping and twisting behavior of the gripper, which is found to be in good agreement with the experimental results. The gripper can pick up a glass ball weighing 22 g, along with many other objects with complicated geometries, under an input pressure of 70 kPa. It can also twist a ping-pong ball by 18° while grasping it. All the grasping and twisting manipulations can be performed within seconds. In contrast to existing techniques for dexterous pneumatic grasping, this soft gripper (1) operates with only a single internal air pressure and (2) uses electrically stimulated ligaments to control the direction of

[1]Mechanical Engineering Department, University of Nevada, Reno, Nevada.
[2]Mechanical Engineering Department, Carnegie Mellon University, Pittsburgh, Pennsylvania.
*These authors contributed equally to this work.

11. Shepherd RF, Ilievski F, Choi W, Morin SA, Stokes AA, Mazzeo AD, *et al.* Multigait soft robot. Proc Nat Acad Sci 2011;108:20400–20403.
12. Robinson G, Davies JBC. Continuum robots-a state of the art. Proc IEEE Int Conf Robot Autom 1991;4:2849–2854.
13. Suzumori K, Iikura S, Tanaka H. Development of flexible microactuator and its application to robotic mechanism. Proceedings of 1991 IEEE International Conference on Robotics and Automation, Sacramento, CA.
14. Kwok SW, Morin SA, Mosadegh B, So JH, Shepherd RF, Martinez RV, *et al.* Magnetic assembly of soft robots with hard components. Adv Funct Mater 2014;24:2180–2187.
15. Brown E, Rodenberg N, Amend J, Mozeika A, Steltz E, Zakin MR, *et al.* Universal robotic gripper based on the jamming of granular material. Proc Nat Acad Sci 2010;107:18809–18814.
16. Kofod G, Wirges W, Paajanen M, Bauer S. Energy minimization for self-organized structure formation and actuation. Appl Phys Lett 2007;90:081916.
17. Araromi OA, Gavrilovich I, Shintake J, Rosset S, Richard M, Gass V, *et al.* Rollable multisegment dielectric elastomer minimum energy structures for a deployable microsatellite gripper. IEEE/ASME Trans Mechatron 2015;20:438–446.
18. Shan S, Bertoldi K, Clarke DR. Dielectric elastomer based grippers for soft robotics. Adv Mat 2015;27:6814–6819.
19. Suo Z. Theory of dielectric elastomers. Acta Mechanica Solida Sinica 2010;23:549–578.
20. Shintake J, Rosset S, Schubert B, Floreano D, Shea H. Versatile soft grippers with intrinsic electroadhesion based on multifunctional polymer actuators. Adv Mater 2016;28:231–238.
21. Yoshimi T, Iwata N, Mizukawa M, Ando Y. Picking up operation of thin objects by robot arm with two fingered parallel soft gripper. In: IEEE Workshop on Advanced Robotics and its Social Impacts (ARSO), Munich, 2012, pp. 7–12.
22. Giannaccini ME, Georgilas I, Horsfield I, Peiris B, Lenz A, Pipe AG, *et al.* A variable compliance, soft gripper. Autonomous Robots 2014;36:93–107.
23. Cheng NG, Lobovsky MB, Keating SJ, Setapen AM, Gero KI, Hosoi AE, *et al.* Design and analysis of a robust, low-cost, highly articulated manipulator enabled by jamming of granular media. In: IEEE International Conference on Robotics and Automation (ICRA), Saint Paul, MN, 2012, pp. 4328–4333.
24. Kim S, Wu J, Carlson A, Jin SH, Kovalsky A, Glass P, *et al.* Microstructured elastomeric surfaces with reversible adhesion and examples of their use in deterministic assembly by transfer printing. Proc Nat Acad Sci 2010; 107:17095–17100.
25. Song S, Sitti M. Soft grippers using micro-fibrillar adhesives for transfer printing. Adv Mater 2014;26:4901–4906.
26. Song S, Majidi C, Sitti M. Geckogripper: A soft, inflatable robotic gripper using gecko-inspired elastomer micro-fiber adhesives. In: Proceedings of the IEEE/RSJ International Conference on Intelligent Robots and Systems (IROS), 2014, pp. 4624–4629.
27. Anderson IA, Gisby TA, McKay TG, Obrien BM, Calius EP. Multi-functional dielectric elastomer artificial muscles for soft and smart machines. J Appl Phys 2012;112:041101.
28. Shan W, Lu T, Wang Z, Majidi C. Thermal analysis and design of a multi-layered rigidity tunable composite. Int J Heat Mass Trans 2013;66:271–278.
29. Shan W, Lu T, Majidi C. Soft-matter composites with electrically tunable elastic rigidity. Smart Mater Struct 2013;22: 085005.
30. Follador M, Cianchetti M, Arienti A, Laschi C. A general method for the design and fabrication of shape memory alloy active spring actuators. Smart Mater Struct 2012;21:115029.
31. Varga Z, Filipcsei G, Zrinyi M. Magnetic field sensitive functional elastomers with tuneable elastic modulus. Polymer 2006;47:227–233.
32. Shiva A, Stilli A, Noh Y, Faragasso A, De Falco I, Gerboni G, *et al.* Ligament-based stiffening for a pneumatically actuated soft manipulator 2016;1:632–637.
33. Maeda S, Hara Y, Sakai T, Yoshida R, Hashimoto S. Self-walking gel. Adv Mater 2007;19:3480–3484.
34. Shan W, Diller S, Tutcuoglu A, Majidi C. Rigidity-tuning conductive elastomer. Smart Mater Struct 2015;24:065001.
35. Finney RH. Finite Element Analysis (Engineering with Rubber, Third Edition) Gent AN. (Ed). Hanser, 2012, pp. 295–343.
36. Tutcuoglu A, Majidi C, Shan W. Nonlinear thermal parameter estimation for embedded internal Joule heaters. Int J Heat Mass Trans 2016;97:412–421.

Address correspondence to:
Wanliang Shan
Mechanical Engineering Department
University of Nevada
1664 N. Virginia St., MS 0312
Reno, NV 89557

E-mail: wshan@unr.edu